October 1965

Midterm Report

# CRYOGENIC MAGNETOMETER DEVELOPMENT

Prepared for

National Aeronautics and Space Administration
Ames Research Center
Moffett Field, California

Contract NAS2-2088

by W. S. Goree

SRI Project PHU-5093

TABLE OF CONTENTS

INTRODUCTION

BACKGROUND

- Magnetometer
- Magnetic Shield

EXPERIMENTAL STUDIES

- Magnetometer
- Magnetic Shield
- Long-Term Stability of the Ames Flux Gate Sensors
- Conclusions of the Long-Term Stability Test
- Temperature Sensitivity of the Ames Sensors
- Results

MEETING WITH HONEYWELL REPRESENTATIVES

FUTURE WORK



Copy No. 6

## INTRODUCTION

This report describes progress made during the first 14 months (July 1964 through September 1965) of a research contract whose objective is the adaptation of a new superconducting circuit to make a magnetometer capable of measuring a rectangular component of small magnetic fields with $10^{-6}$-gauss resolution or better. A concurrent aim of the work is to use a superconducting magnetic shield to produce a low field region suitable for testing the superconducting magnetometer (which must operate at liquid helium temperatures) as well as room temperature magnetometer probes. Additional aims are to consider the application of quantized flux, the Josephson effect, and other superconducting phenomena to instruments other than magnetometers.

The Background section of this report covers the basic principles of the superconducting magnetometer and magnetic shield as well as the present magnetometer and shield design. The majority of the experimental studies, presented in the Experimental section, were done since the distribution of our March 1965 report. Recommendations and designs of superconducting magnetic shielding were discussed with representatives from the Honeywell Company as requested by NASA Ames. A review of our discussion is given in the third section of this report. Our plans for future work are presented in the final section of this report.

## BACKGROUND

### Magnetometer

Several properties give superconductors unique advantages for very sensitive measurements of magnetic fields. These properties are:

1. Zero electrical resistance, which allows persistent currents, that is, currents that flow undiminished forever in a closed superconducting circuit.

2. The Meissner effect, which is the expulsion of the magnetic field from the interior of a solid superconductor when it is cooled below its superconducting transition temperature in the presence of a magnetic field.

3. Quantized magnetic flux trapped in superconducting loops. The only possible values of magnetic flux trapped inside a closed superconducting loop are integral multiples of $hc/2e = 2\times10^{-7}$ gauss $cm^2$.

This last property of superconductors, which was recently verified experimentally for the first time at Stanford University[1] (it was pre-

[1] Deaver, B.S.,Jr.,and Wm.M.Fairbank, Phys.Rev.Letters 7, 43 (1961)

dicted by Fritz London about 1948), can be used in principle to (1) produce a region of zero magnetic field and (2) measure very small magnetic fields. When a loop of superconducting material is cooled below its transition temperature in the presence of a magnetic field producing an arbitrary amount of magnetic flux inside the loop, a current which causes the flux inside the loop to become quantized at the nearest integral value of $hc/2e$ is induced in the loop. Thus, if a loop is cooled in a magnetic field which produces less than one-half a flux unit through the loop, a current will be induced which expels all the magnetic flux from the interior of the loop, producing zero flux inside the loop. Further, the current flowing in the loop is proportional to the value of the magnetic field in which the loop was cooled and a measurement of this current constitutes a measurement of the magnetic field.

During the experiments to measure quantized magnetic flux at Stanford University, a new superconducting circuit was originated for observing very small changes in magnetic flux.[2] This circuit can be readily adapted for magnetic field measurements. The circuit is diagrammed in Fig. 1. Coils A and B constitute a single superconducting circuit. The total magnetic flux enclosed by this circuit must be constant in time because the electrical resistance is zero. If an external field is applied, for example to Coil A, thus causing a flux change through this coil, the circuit reacts by producing a current which induces flux changes in Coil A and in Coil B, and the sum of the changes due to this current exactly cancels the external flux change. The induced current will persist forever or until the external field has been removed. The persistent current in the superconducting circuit is a permanent record of the flux change which was attempted. A measurement of this current measures the attempted change in flux.

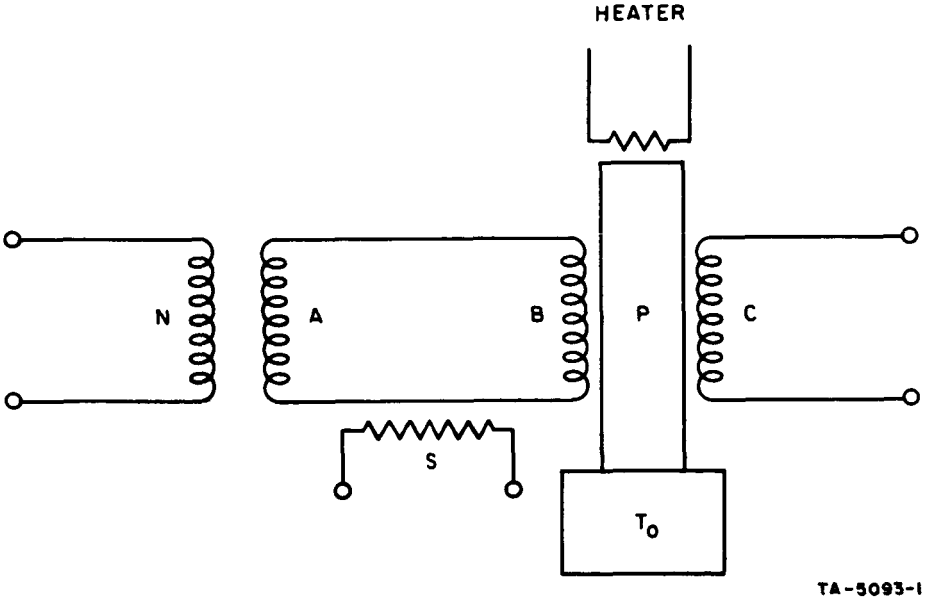


FIG. 1 SUPERCONDUCTING CIRCUIT

[2] Deaver, B. S., Jr. and Wm. M. Fairbank, Proceedings of the Eighth International Conference on Low Temperature Physics. R. O. Davies, ed., Butterworth, Washington, D.C., 1963, p. 116

The operation of the circuit to measure a flux change via the persistent current is as follows. First, any persistent current already present in the circuit AB is eliminated by momentarily heating a small region of the circuit with heater S, causing a normal resistance in that part of the circuit and thus causing any currents to decay to zero. If the circuit is returned by cooling to the superconducting state, then a flux change caused in Coil A by an imposed external field will be balanced by the current induced in the circuit AB. To measure this persistent current, Coil B and a secondary coil, C, are wound around a superconducting modulator, P, which may be a solid post, a thick wall cylinder, etc. The superconducting modulator, P, is thoroughly cooled by contact to a temperature, $T_0$, below its superconducting transition temperature. The modulator can be periodically heated so that it first rises above its superconducting transition temperature and then cools back to the superconducting state. When the modulator is normal (that is, above its superconducting transition temperature), the current flowing in B causes a magnetic flux to link both B and C. When the modulator goes superconducting, the magnetic flux inside the superconductor is expelled because of the Meissner effect, thus changing the amount of flux linking B and C. As the modulator is heated and cooled periodically, the periodic variation of the flux in C causes an alternating voltage across the coil C. This voltage, which can be measured readily, is proportional to the persistent current flowing in the circuit AB and is consequently proportional to the attempted flux change in Coil A.

A somewhat improved measurement is possible by providing an additional coil, N. The current in N will cause the flux through A to change. When the change is exactly equal and opposite to that caused by the external field change which is to be measured, there will be no necessity for a current in the circuit AB; consequently, the signal from C will be zero. At this null condition the current in N is proportional to the field change applied to Coil A.

The circuit and variations of it have been used to measure flux changes of approximately $10^{-8}$ gauss $cm^2$. It can be adapted to a variety of sensitive magnetic measurements.

Using the properties and new circuit techniques described above, we have constructed a sensitive magnetometer with field resolution of better than a microgauss. The complete magnetometer circuit now in operation will be described in detail. Figure 2 is a diagram of the final circuit giving the important dimensions. To make the device more suitable for measuring weak fields, Coil A in Fig. 2 is of rather large cross section and is aligned with the field to be measured. For absolute field measurement Coil A can be flipped through $180^0$ in the field, and the resulting change in flux through Coil A, i.e., twice the total original flux, can be measured as described above. The actual measuring circuit, Coils B and C, and the modulator P are located along the axis of rotation of Coil A.

Because it is the total amount of magnetic flux being swept in and out of the output coil, C in Fig. 2, that determines the output signal

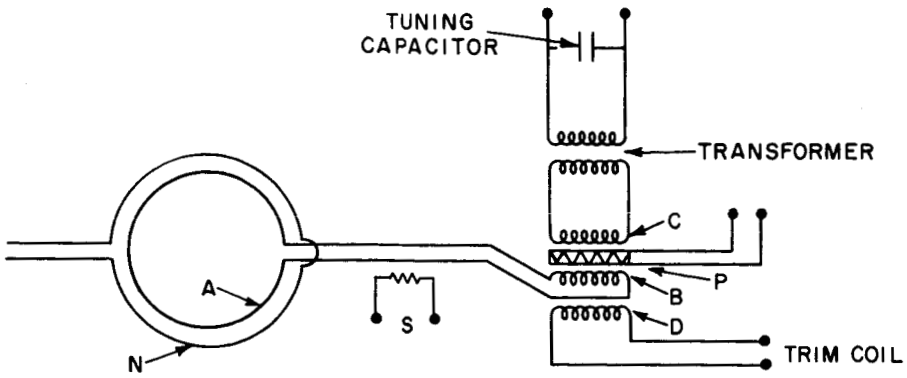


CIRCUIT DATA

1. P is the indium modulator heated by a CuAu layer of 85Ω resistance

2. S is a 30Ω carbon resistance heat switch

3. The tuning capacitor used at 30.3-kc signal frequency was 0.0018 $\mu$f

4. Transformer: Primary is 10 turns of lead-plated copper strip.
   Secondary is 5000 turns of 2-mil niobium wire

5. Coil dimensions:

| Coil | Number of turns (2-mil niobium wire) | Inside Diameter (cm) |
|---|---|---|
| N | 2 | 0.96 |
| A | 2 | 0.96 |
| B | 162 | 0.05 |
| C | 155 | 0.10 |
| D | 150 | 0.15 |

TA-5093-17

FIG. 2 MAGNETOMETER CIRCUIT

and that ultimately limits the magnetic field sensitivity, a modulator of large cross section is required for the measurement of weak fields. However, larger modulators require larger amounts of heating power and are thus somewhat unsatisfactory. In our existing circuit we have compromised with the use of a 0.002-in. OD modulator.

The modulator is a hollow superconducting cylinder heated internally with a CuAu resistance film. The cylinder walls exhibit the Meissner response which is linearly proportional to a changing magnetic field. The hollow cylinder construction is a single turn, closed superconducting loop which exhibits quantized flux response. Quantized flux response is a multivalued function of the applied magnetic field. The output coil, C in Fig. 2, senses the flux change in the loop that occurs as the loop becomes superconducting. If the applied field produces exactly one unit of flux through the loop (or any integral multiple of one unit), no change occurs when the loop is cooled, and there is no output voltage. However, for other applied fields a current is induced in the loop as it becomes superconducting to change the enclosed flux to the nearest quantized value. When the loop is cooled in a field producing less than one-half a flux unit, a current is induced to oppose the applied field and produce zero flux inside the loop. When the loop is cooled in a field producing slightly more than one-half a flux unit, the induced current produces a field in the same direction as the applied field to change the flux to one unit inside the loop. This change gives an output voltage of sign opposite to that for the previous case. The pattern repeats as the field is increased, giving an output voltage which is a periodic function of the field with period $hc/2e$ divided by the area of the loop as shown in Fig. 3. Thus the response from our modulator is a superposition of the linear Meissner effect and the periodic quantized flux effect.

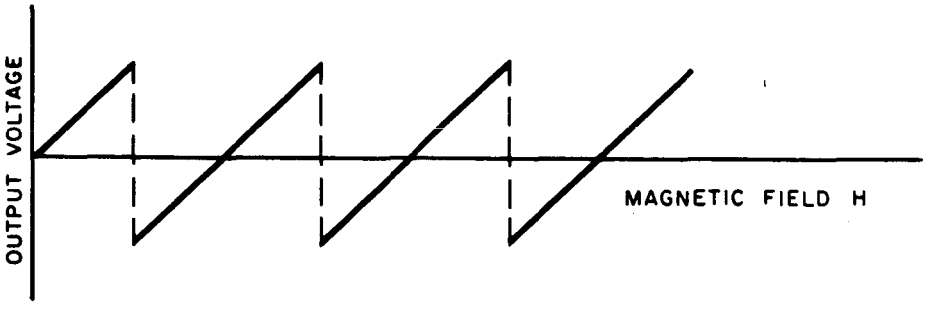


FIG. 3 CIRCUIT RESPONSE WITH SUPERCONDUCTING LOOP

Coil N in Fig. 2 is a null coil whose operation was described earlier. Coil D in Fig. 2 is a trim coil used to zero the magnetic field at the modulator when Circuit AB is open.

Figure 4 is a block diagram of the electronics used with the magnetometer. Figure 5 is a photograph of the completed magnetometer mounted

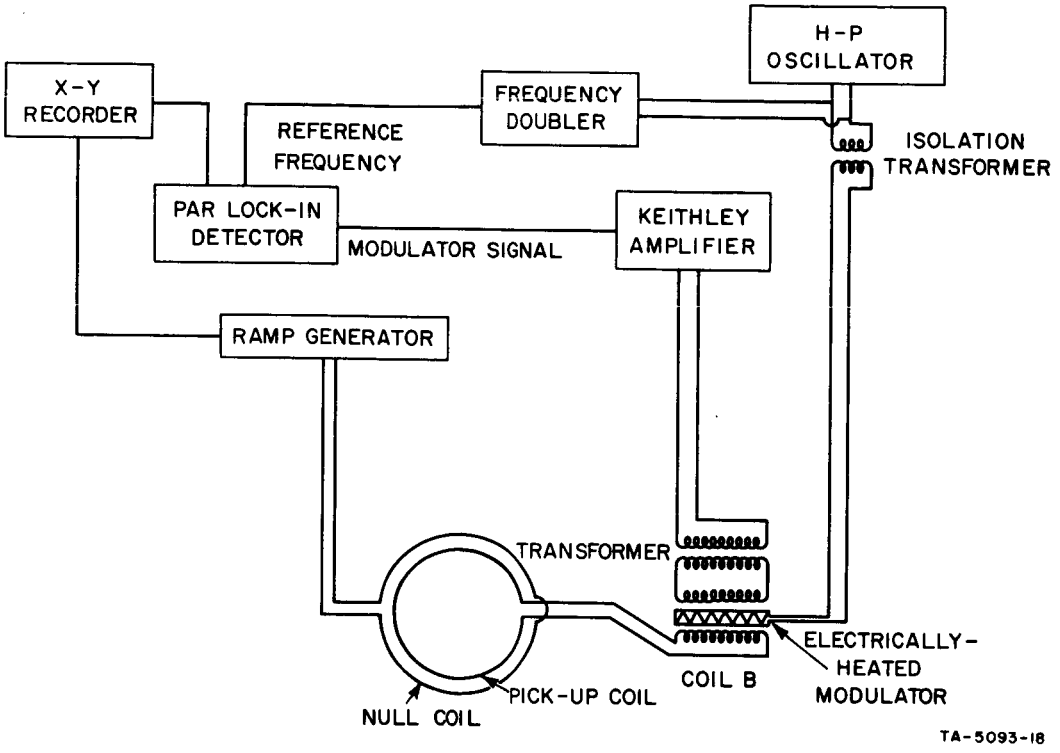


FIG. 4 MAGNETOMETER ELECTRONICS

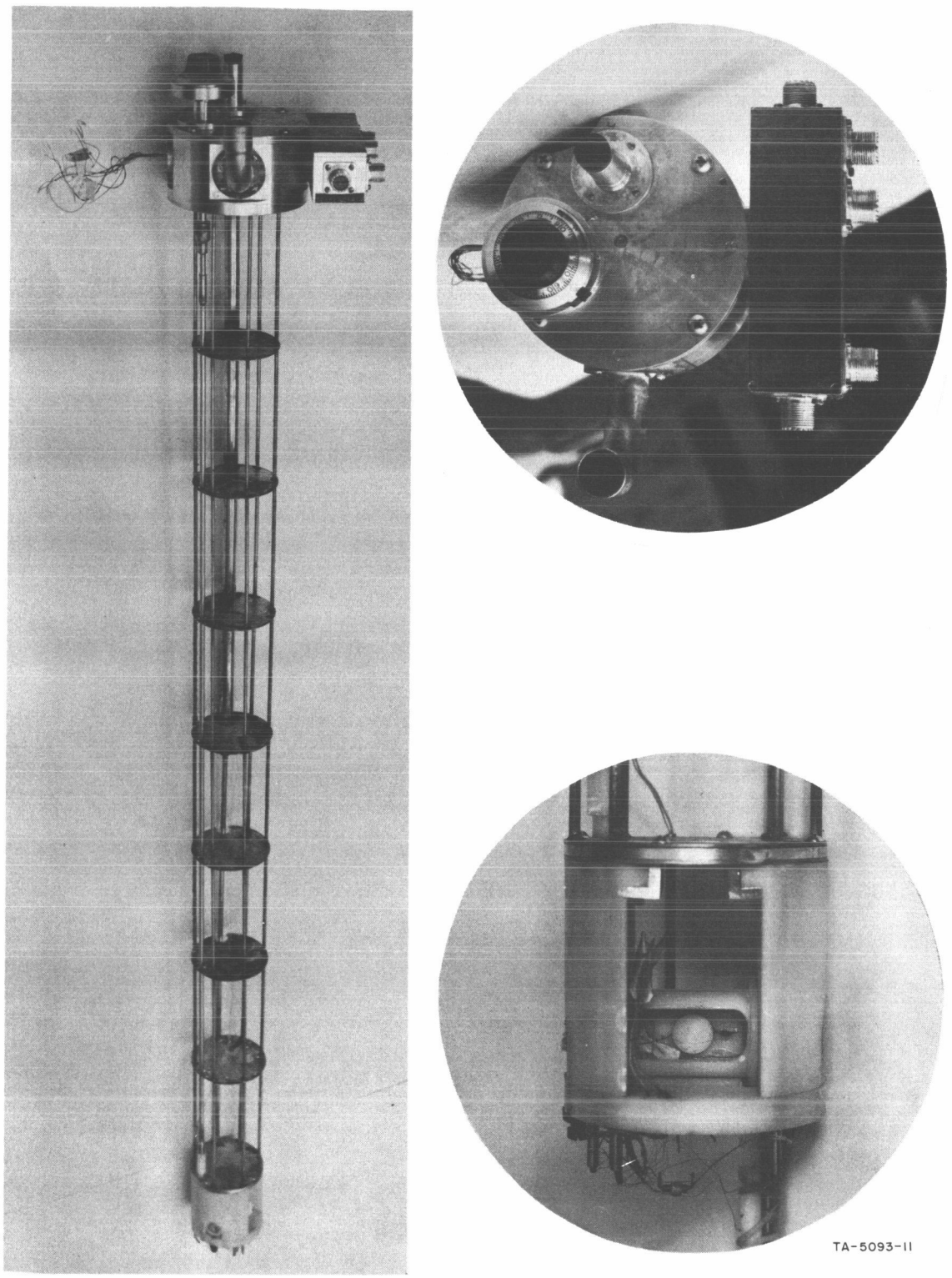


FIG. 5 SUPERCONDUCTING MAGNETOMETER ASSEMBLY

in its test fixture. The magnetometer assembly fits into the 3-in. Linde dewar (Fig. 6) and is designed so that the sensing element is approximately at the axial center of the superconducting shield. Rotation of the pick-up coil through $180^{0}$ for absolute field measurement is provided by a rack and pinion drive made of Delrin. The modulator is mounted along the axis of rotation so that its average field remains constant except for that due to the pick-up coil. Each pair of electrical leads to the various circuit components shown in Fig. 2 passes through one of the $\frac{1}{8}$-in. OD BeCu support tubes to provide good shielding from electrical pick up.

Magnetic Shield

In order to test the magnetometer circuit it is necessary to have a very low magnetic field region. It would be most desirable to have the total field in the region below $10^{-6}$ gauss; however, it may be sufficient to have a region in which one component of the field can be varied smoothly through zero in $10^{-6}$-gauss increments. As mentioned in the introduction, it was decided that it is highly desirable that the low field region be suitable for testing both the superconducting circuit and room temperature magnetometers, i.e., the Ames flux gate probes, to make it more generally useful and to provide for comparison tests.

Superconductors offer several very unique advantages in magnetic shielding. The zero resistance property and the Meissner effect provide a superconductor with a self-regulating mechanism for cancelling magnetic fields,a-c or d-c, which attempt to penetrate its boundary. The quantized flux property can, in principle, allow one to achieve absolute zero fields. Consider, for example, a volume enclosed by a superconducting shell initially above its transition temperature. If the total magnetic flux passing through this volume is less than one-half of a flux unit, $<hc/4e$, and the superconducting shell is cooled below its transition temperature, then currents will be induced in the shell to exactly cancel the contained magnetic flux leaving a volume of truly zero magnetic field. This latter possibility is beyond the needs of our proposed research. We are more concerned with field stability and low fields in the microgauss range.

Mercereau[3] has shown that superconducting cylinders provide extremely stable magnetic field environments and further that the radial component of the external field passing through the cylinder wall can be substantially reduced by rotating the superconductor about its longitudinal axis as it is cooled through its superconducting transition temperature region. When the resistance of the metal is very low but before it is superconducting, induced eddy currents tend to cancel the radial field. Once the cylinder is superconducting, its rotation may be stopped and the zero resistance maintains the reduced radial field. Mercereau used a small

---

[3] Vant-Hull, L. L. and J. E. Mercereau, Magnetic Shielding by a Super-Conducting Cylinder, Rev. Sci. Inst. 34(11), 1238 (1963)

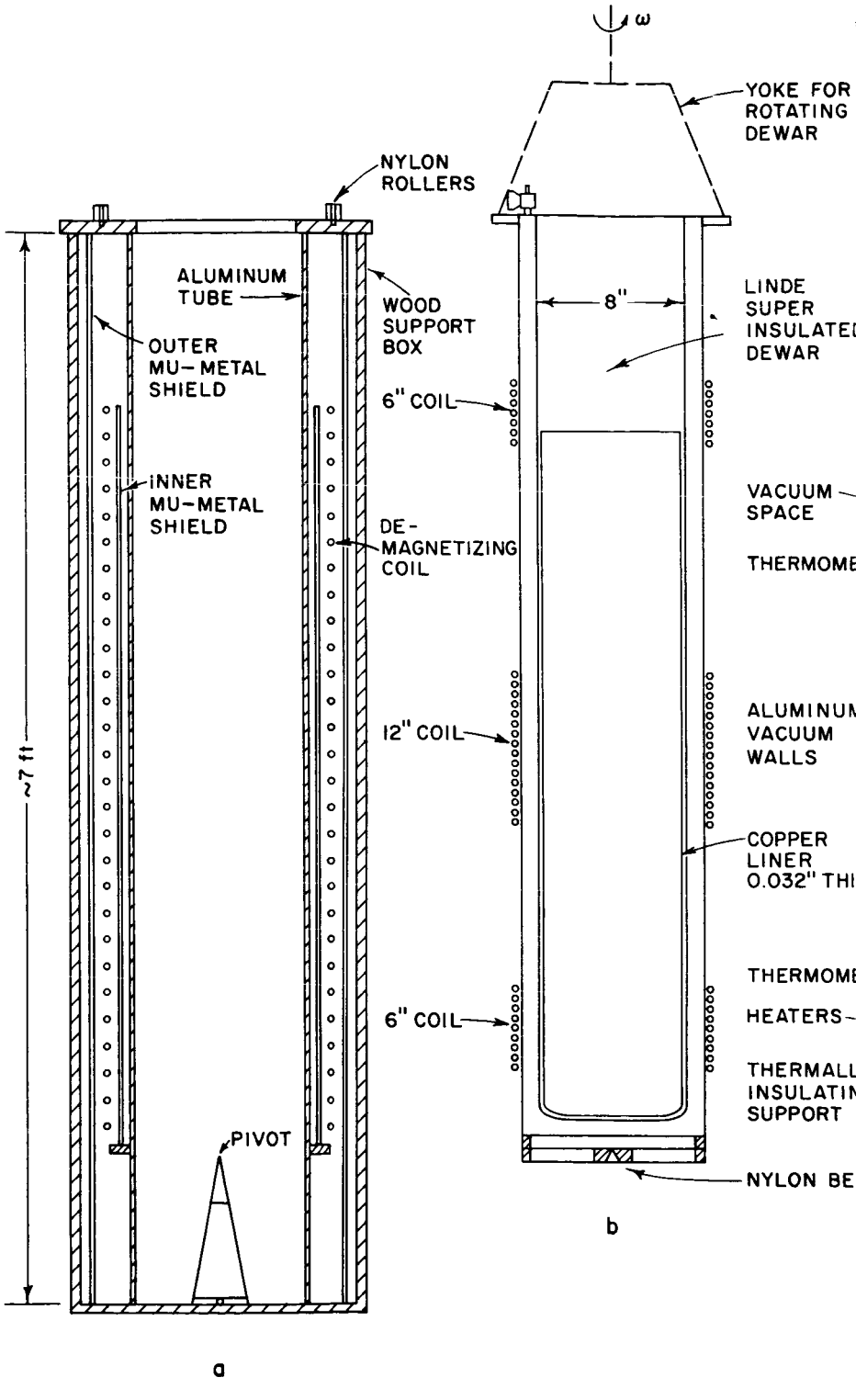


FIG. 6 MAGNETIC

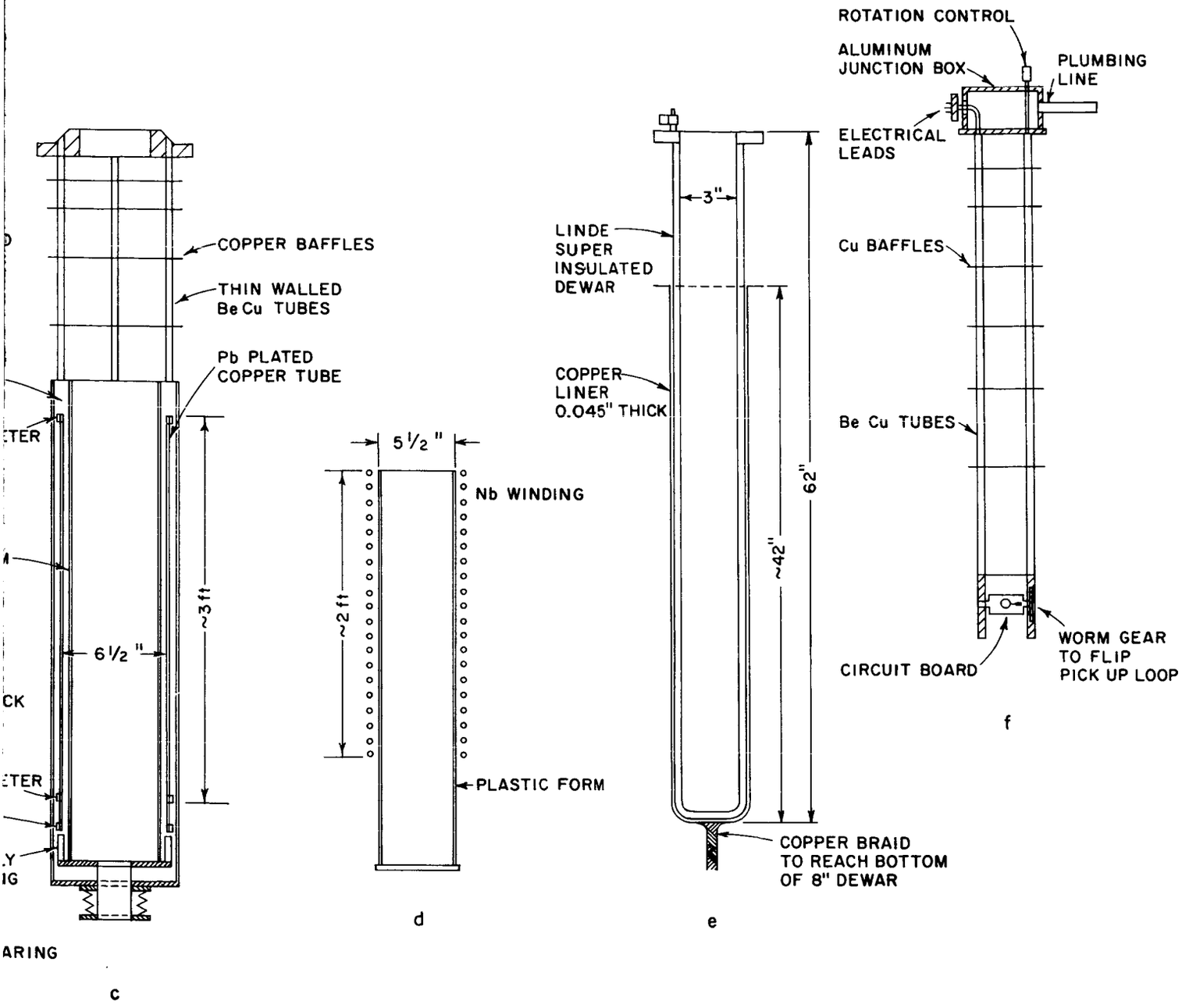


RC-5093-5

SHIELD, TESTING CRYOSTAT, AND MAGNETOMETER ASSEMBLY

tin cylinder (1-in. OD by 6-in. long) in his experiments and rotated the cylinder directly in a liquid helium bath which was temperature regulated.

The requirements of this research, i.e., a room temperature access into the low field environment suitable for testing the Ames flux gate sensor, necessitated a much larger shield assembly than the one described by Mercereau. In designing and building this larger shield we were faced with several uncertainties such as scale factors in going from a very small to a large shield, most suitable material, and optimum geometry.

Because operation of a magnetic shield was an adjunct to the main object of the research, the operation of a sensitive magnetometer based on superconductivity, we decided that the shield should be relatively simple yet offer the possibility of trying various superconducting materials. The complete magnetic shield assembly now in operation will be described in detail. Figure 6 is a line drawing of the magnetic shield assembly.

The outermost shield is a thoroughly annealed Mu-metal cylinder 84-in. long, $13\frac{1}{2}$-in. diameter, with 0.050-in. thick walls. A second annealed Mu-metal cylinder 60-in. long, $12\frac{1}{2}$-in. diameter, with 0.050-in. walls is centered within the first cylinder. This shield is wound with a coil so that an alternating field can be applied immediately prior to operation to demagnetize the inner cylinder. These shields should reduce the field in the central volume to $10^{-4}$ gauss or less.

Within this region a superconducting cylinder (actually a Pb coating 0.004-in. thick by 36-in. long electroplated onto a pure copper tube $6\frac{1}{2}$-in. OD with 0.030-in. walls) is placed inside a liquid helium dewar (Fig. 6b). The lead cylinder is mounted inside a vacuum jacket (Fig. 6c) so that it can be cooled slowly through the transition temperature of $\sim 7^{\circ}$K. Heaters and thermometers are mounted on the cylinder to control and monitor the cooling rate.

The liquid helium dewar (Fig. 6b) is 8-in. ID and about 68-in. long and was specially constructed by the Linde Company, using their super-insulation so that no liquid nitrogen jacket is required. It is made entirely of nonmagnetic material, primarily aluminum and fiberglass. As depicted in Fig. 6, the dewar is supported on a pivot at the bottom and has nylon rollers around the top flange, so that it and its contents can be rotated about a vertical axis at speeds up to about 60 rpm. The aluminum alloy of the dewar wall is a poor thermal conductor at liquid helium temperatures; thus the copper liners inside the 8-in. dewar and outside the 3-in. dewar walls are necessary to maintain low thermal gradients along the shield as the liquid helium level falls.

In operation the dewar is rotated as the lead cylinder is cooled through its transition temperature. When the resistivity of the cylinder is low but not yet zero, the rotation will reduce the radial field components due to eddy currents induced in the cylinder. Then when the lead cylinder becomes superconducting, it will freeze in a small,

essentially axial field. Since no flux changes can occur through the superconducting wall, the residual field is extremely stable.

A final reduction of the axial field is made by passing a small current through a superconducting solenoid (Fig. 6d) which is 24-in. long and wound with 0.010-in. Nb wire. This solenoid is fitted with a d-c transformer to give vernier control of the field after the solenoid current is persistent. Field regulation with this transformer is about $10^4$ times more sensitive than the regulation possible with the solenoid alone.

The test region is isolated from the main liquid helium bath by a second Linde superinsulated dewar, 3-in. ID and about 62-in. long. The cryostat for testing the superconducting magnetometer is placed in this dewar and the dewar filled with liquid helium. The temperature is lowered by pumping on the bath and controlled by regulating the pressure above the bath.

For testing room temperature devices, the dewar is left open to the room or temperature compensated for thermal loss to the main helium bath.

Because the shield assembly was to be used for long-term stability tests, we decided to use lead as the superconducting shielding material. The rather high transition temperature for lead ($7.2^{\circ}$K) enables the helium bath to be maintained at atmospheric pressure, thereby allowing topping up of the bath without appreciably changing the shield temperature. The use of indium or tin, although possibly better shield materials, would require elaborate helium transfer methods or closed cycle helium refrigerators to maintain the shield below its transition temperature during continuous long-term experiments.

## EXPERIMENTAL STUDIES

### Magnetometer

Two experimental tests of the magnetometer have been made. In both tests we used hollow indium modulators heated internally by a CuAu resistive film. This type of modulator should exhibit both the Meissner effect and quantized flux response. In the first experiment an apparent electrical short between the indium and the heater limited the modulator heater frequency to about 1000 cps. Also the noise level was too high to detect quantized flux response. The Meissner effect was observable and the noise level was measured at $\pm 7 \times 10^{-5}$ gauss. The second experiment used a better indium modulator and considerably better experimental results were obtained. This experiment will now be described in detail.

At the beginning of the experiment the superconducting shield was cooled in the usual manner, the Mu-metal was depermed, and the magnetic test environment shown in Fig. 7 was locked in. This figure also shows the position of the superconducting magnetometer circuit during these studies.

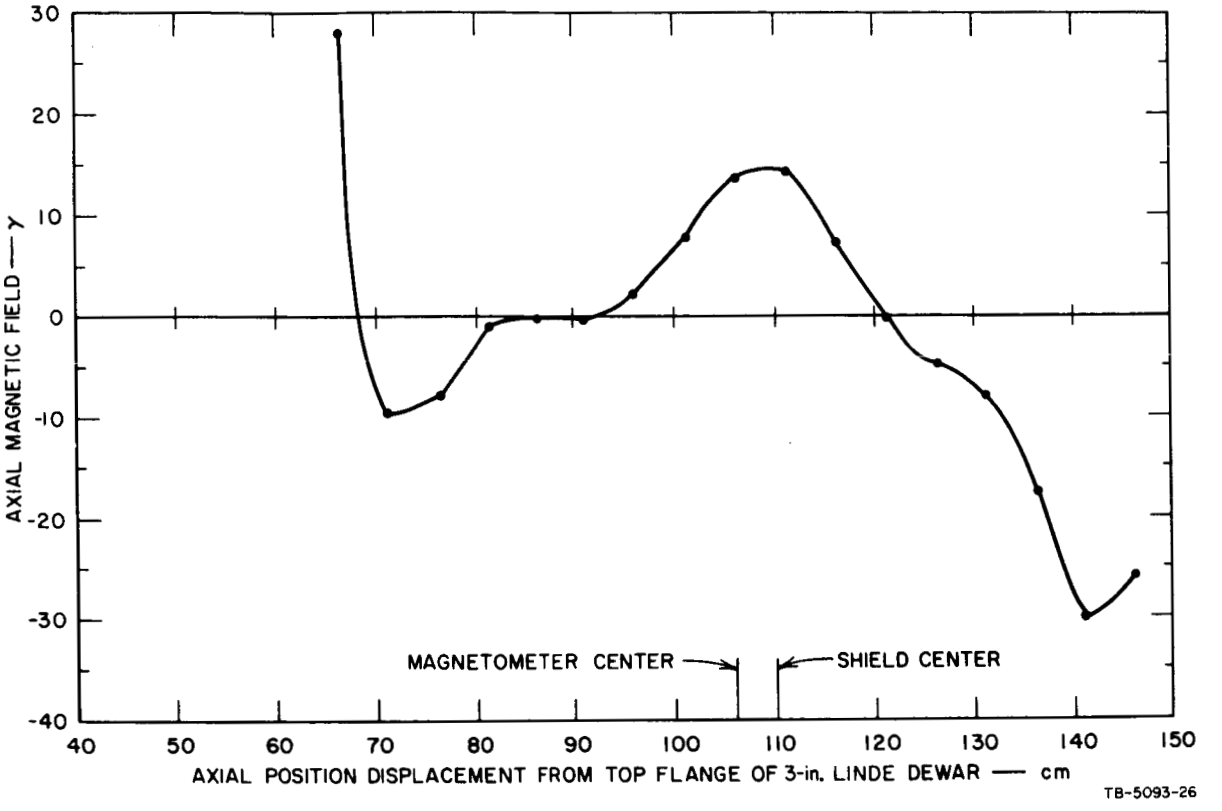


FIG. 7 AXIAL MAGNETIC FIELD MAP AT THE BEGINNING OF THE SUPERCONDUCTING MAGNETOMETER EXPERIMENT

The initial test of the magnetometer circuit consisted of a series of studies of the output signal from the magnetometer versus the applied modulator voltage for different bath temperatures. The results were plotted as shown in Figs. 8 and 9. Our studies were made at the ambient field condition shown on Fig. 7. Different fields change the signal amplitude due to changes in the flux at the modulator. The major significance of these data is that they seem to indicate the quality of the superconducting modulator. This quality factor is best understood by reference to Figs. 8, 9, and 10. In Fig. 8 the bath temperature, T, is above the superconducting transition temperature, $T_c$, for indium (i.e., $>3.37^{\circ}K$). In this case the heating current to the modulator provides no movement of flux due to either the Meissner effect or quantized flux and any output signal is due to noise picked up from the heater current, etc.

Figure 9 is for $T < T_c$. As we start increasing the power from zero, we observe no initial output because none of the indium layer is being heated above its transition temperature. With further increase in power, parts of the indium begin to switch on and off, i.e., are taken above and below their superconducting transition temperature. This initial signal is caused by the Meissner effect moving magnetic flux in and out of the indium layer. With further increase in power we should reach a power range where the entire indium layer is switched uniformly. At this point the signal is from the Meissner effect and quantized flux. Further power increases cause parts of the modulator to remain above $T_c$ and thus reduce the output signal. At these higher powers, the slope of the output signal should decrease, due to a decreasing Meissner effect, but periodic quantized flux should still appear. Finally, the heat input to the modulator is sufficient to cause all of the superconducting layer of indium to remain above $T_c$, and the output signal should return to its zero power level.

For decreasing power the cycles should repeat with no hysteresis, if the initial field inside the hollow superconducting post was the same as the initial external field. The observed hysteresis and erratic power plots obtained with our modulator (Fig. 9) are believed to be due to electrical shorts between the superconducting indium and the CuAu heater or nonuniform thermal contact of the indium with the heater or the helium bath. Inspection of region "a" in Fig. 9 shows that even if one is able to find a power giving optimum signal, this power will be crucial and require accurate, stable control.

These power plots are to be compared with an "ideal" plot shown in Fig. 10. This ideal plot is based on experience with similar modulators at Stanford University. There a large number of modulators were studied, and power plots of the type shown in Fig. 10 were generally obtained from modulators with no electrical shorts and with a uniform superconducting layer.

We made numerous power plots at various bath temperatures from above $T_c$ for indium ($= 3.37^{\circ}K$) to below the liquid helium lambda point ($2.19^{\circ}K$). In general more power is required to initiate switching of the indium cylinder at lower temperatures. The erratic signal continued at all

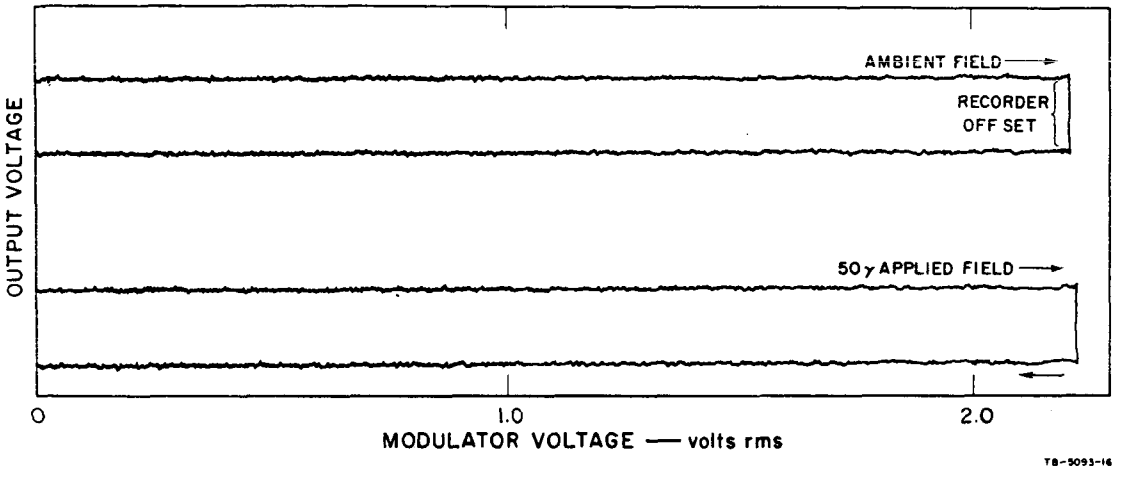


FIG. 8 MAGNETOMETER OUTPUT VOLTAGE VERSUS MODULATOR HEATER VOLTAGE (Bath Temperature $>T_c$)

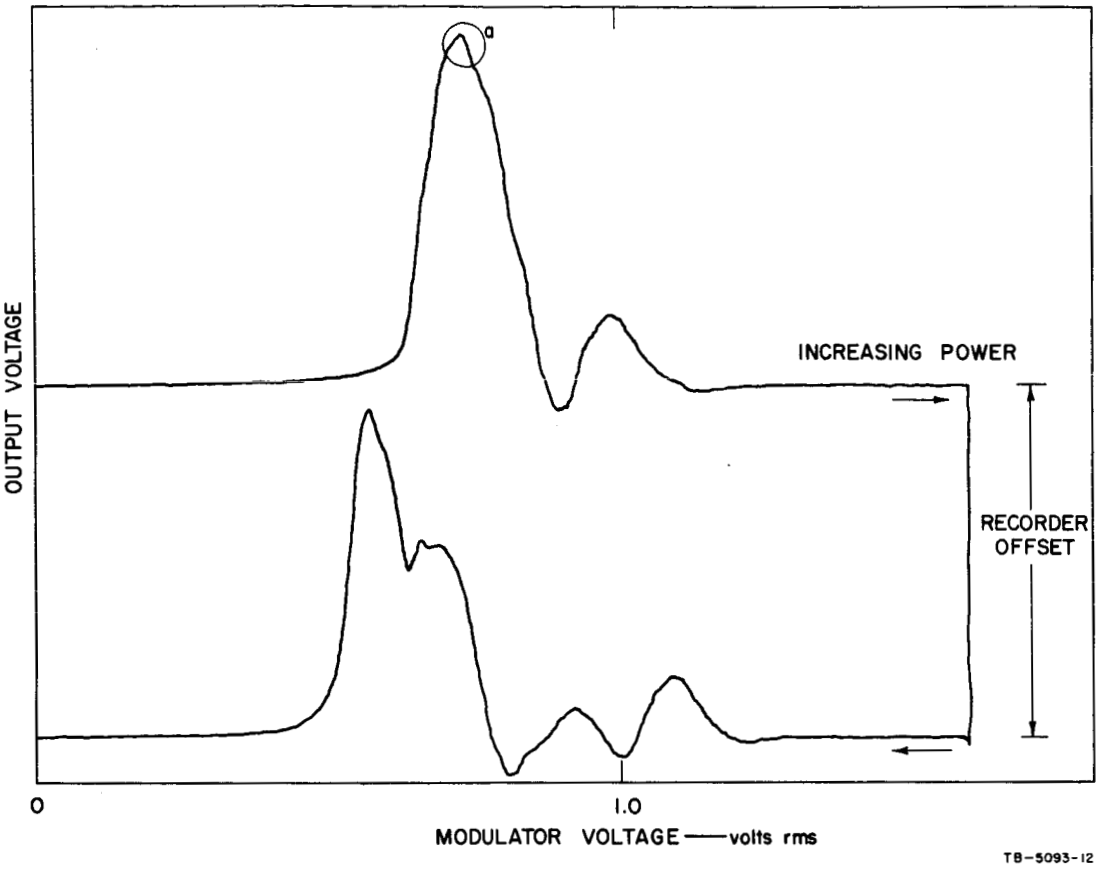


FIG. 9 MAGNETOMETER OUTPUT VOLTAGE VERSUS MODULATOR HEATER VOLTAGE (Bath Temperature Regulated at 3.23°K)

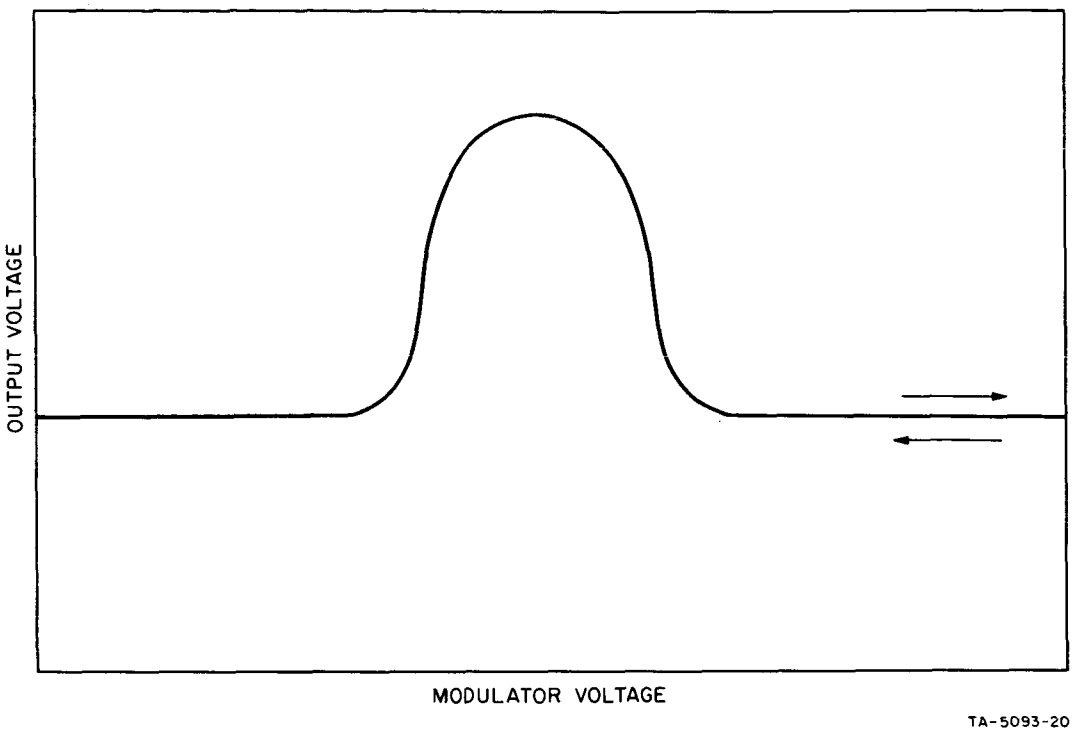


FIG. 10 IDEAL PLOT OF MAGNETOMETER OUTPUT VOLTAGE VERSUS MODULATOR HEATER VOLTAGE (Bath Temperature $<T_c$)

temperatures studied. However, we found that temperatures around 2.5°K gave the best signal and chose this range to measure the quantized flux response.

Before measuring the quantized flux signal we capacitively tuned the output signal from the magnetometer and tried various frequencies so that we could select that frequency giving the maximum signal. The modulator could be switched at frequencies up to 100 kcps although the maximum signal was observed at 30.3 kcps, which frequency was chosen for the initial studies.

The quantized flux studies were made by stabilizing the helium bath temperature, fixing the modulator power, then sweeping the magnetic field at the modulator using the null coil (Coil N, Fig. 2) driven with a current ramp generator. Plots of signal voltage versus applied magnetic field were then made using the modulator power as a parameter. Figure 11 shows a number of these plots of signal versus field made at different modulator power settings. We find that at low power the signal is not a function of applied field. As power is increased the signal begins to vary approximately linearly, which is characteristic of the Meissner effect modulator. Additional heating switches more of the modulator and increases the signal. Finally, we reach the power setting where the entire modulator switches and the quantized flux response is superimposed on the Meissner effect. At this power setting we made sensitivity and noise studies. Three traces of the signal versus field plot were made to check signal stability, and then the null field was set at point "a" (Fig. 12). Expanding the Y-scale and changing the X-axis to time, we obtained a zero trace; then by using the large Nb solenoid associated with the superconducting shield, we applied a $\pm$1.079 gamma field to the pick-up coil (A in Fig. 4). The response is shown in Fig. 12 where we see that 2.158 gamma corresponds to approximately 24 divisions and the noise is approximately 1 division. This gives a magnetic field resolution of better than 0.1 gamma. It should be noted that the magnetic field at the superconducting modulator corresponding to one quantum of flux is approximately 12 mgauss. The amplification of field by the circuit AB, Fig. 2, is approximately 50, so a field change of about 0.24 mgauss (i.e., 24 gamma) is required to produce a quantum of flux at the modulator.

We draw the following conclusions from these data:

1. It is possible to observe quantized flux with our circuit, and the sensitivity of the superconducting magnetometer is better than 0.1 gamma.

2. The performance of the magnetometer circuit indicates that the coupling between the modulator and the pick-up coil is good, that electrical pick up from the modulator is not severe, and that the superconducting transformer in the output circuit is well matched.

3. The indium modulator can be switched at frequencies up to 100 kcps.

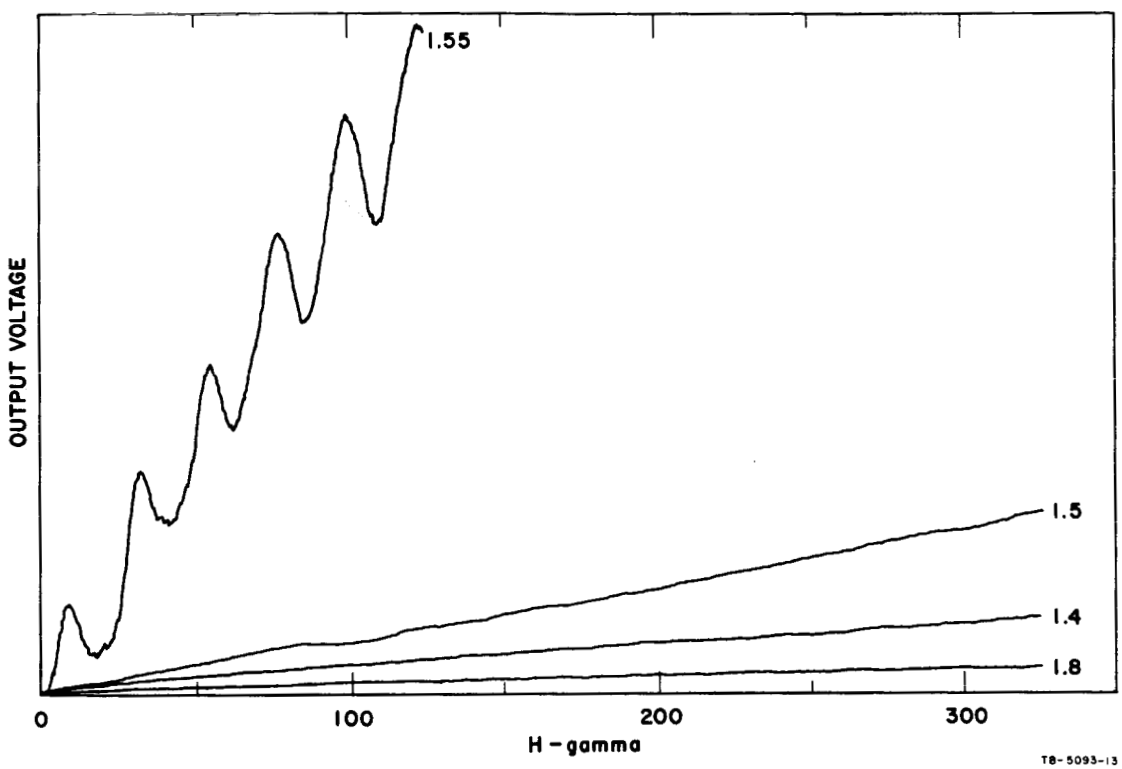


FIG. 11 MAGNETOMETER RESPONSE VERSUS APPLIED MAGNETIC FIELD

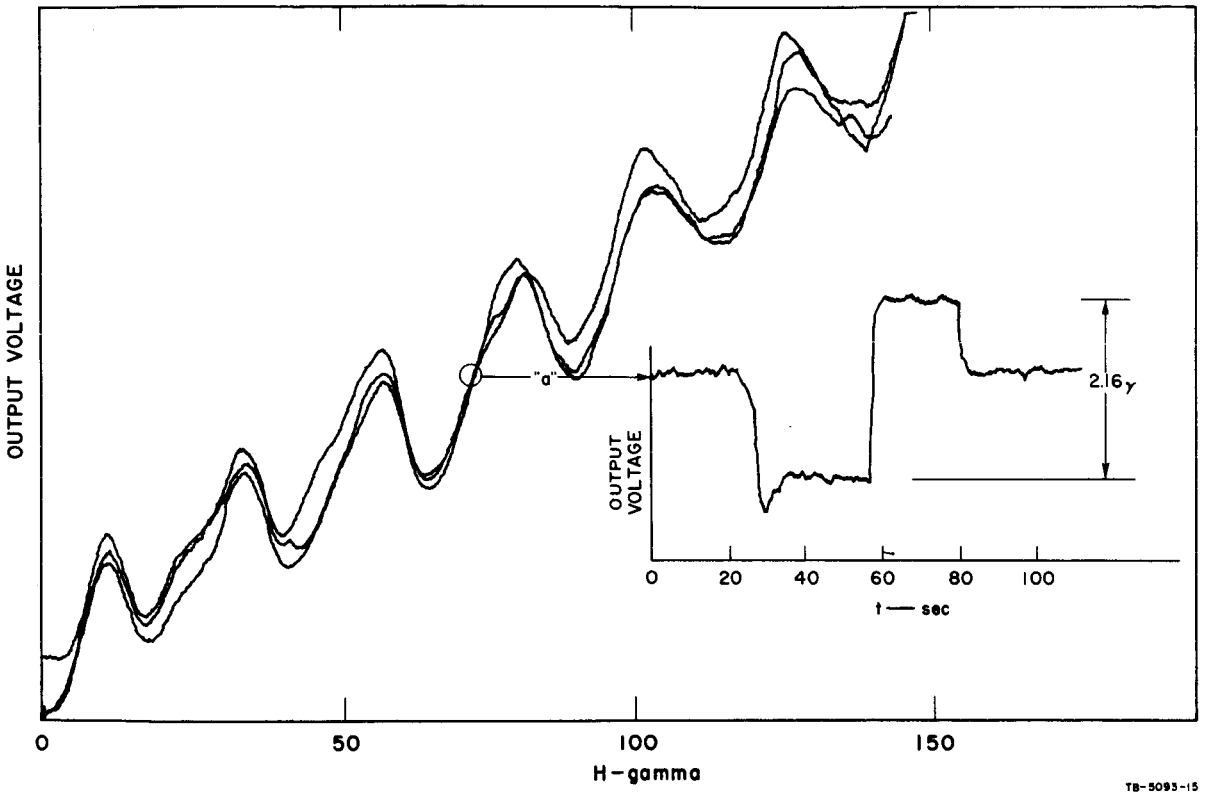


FIG. 12 MAGNETOMETER RESPONSE VERSUS APPLIED MAGNETIC FIELD AND FIELD SENSITIVITY MEASUREMENT

4. A comparison of the experimental power plot (Fig. 9) with the theoretical one (Fig. 10) indicates that the modulator used in these experiments was not ideal. Improvements in the modulator should improve stability, signal to noise, and sensitivity.

5. All of the significant difficulties apparent in the magnetometer performance were caused by the superconducting modulator. These were (a) lack of reproducibility of signal, (b) unstable power point for maximum signal, (c) short modulator life unless it is kept at liquid helium temperature.

Magnetic Shield

The magnetic shield has been assembled and used numerous times at liquid helium temperatures. Careful studies have been made of the effects of deperming the Mu-metal, helium boil-off rates, magnetic field attenuation of the superconducting shield, the effect of shield rotation during cooling on the "locked in" axial magnetic field gradients, and long-term stability.

Deperming of the inner Mu-metal shield gave very unpredictable residual axial magnetic fields. Numerous 60-cycle, a-c deperms were tried with currents from 1/4 amp to a maximum of 10 amps. Also different combinations of current and rate of current decrease were used. In general, currents of about 2 amps rms which were linearly decreased from maximum to zero in 30 sec gave the best results, but in no case could we deduce any consistent reproducible pattern of deperm procedure versus resultant field. Typical examples of the axial magnetic field of the Mu-metal before and after various deperming procedures are shown in Fig. 13.

The average helium boil-off rate with the 3-in. Linde dewar at room temperature was approximately 0.5 liter/hr. With the 3-in. dewar at helium temperature, this was reduced to 0.3 liter/hr. These rates are very low for such large, straight-wall dewar systems and are satisfactory for long-term operation.

Several experiments were performed to study the effect of rotating the superconducting magnetic shield as it cooled through its transition temperature region. As discussed earlier, the induced eddy currents are supposed to cancel radial magnetic field components and leave a very homogeneous axial magnetic field inside the shield. This axial field may then be controlled with a persistent current solenoid. In all experiments the shield was rotated at approximately 1 rps about its vertical axis in the relatively low field environment of the double Mu-metal shields. Axial field maps were made before and after each rotation experiment, and the effect of eddy current shielding was evaluated by comparing the axial magnetic field gradients before and after rotation. The superconducting transition for the lead shield occurred over about 10 millidegrees; cooling times through this temperature range were varied from a few seconds to as high as 20 sec. In no case could any change in the axial magnetic field gradients be detected as a function of the

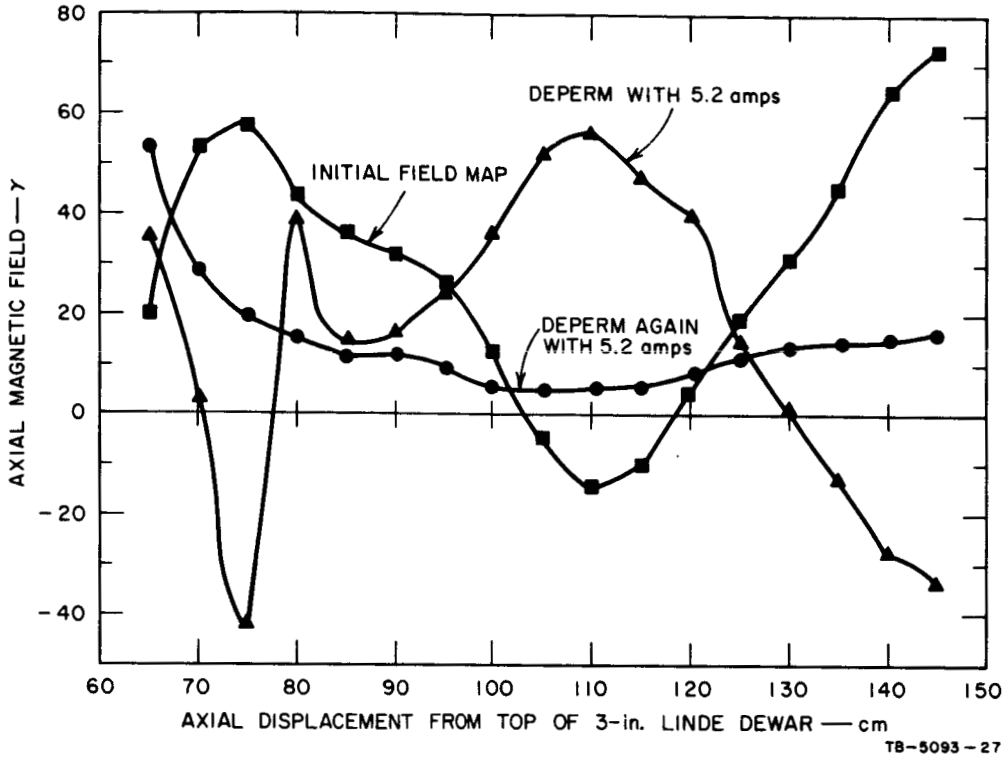


FIG. 13 EXAMPLES OF THE EFFECT OF DEPERMING THE MU-METAL SHIELD

rotation procedure. This problem has not been investigated extensively because the shield assembly is perfectly adequate for its current use.

We do feel that much slower cooling rates as well as a thicker lead superconducting layer would show more pronounced rotation effects. Also, superconducting materials such as tin or indium, with much lower normal resistance immediately before the superconducting transition, would be more ideally suited for eddy current damping than is lead.

The magnetic field attenuation of the superconducting shield has been measured by hoisting the entire 8-in. dewar assembly out of the Mu-metal shields and applying external magnetic fields with coils wrapped on the outside of the dewar. In one test the Ames sensor was located at the center of the superconducting shield and external magnetic fields were applied using the 12-in. and the upper 6-in. coils wound on the outside of the large dewar (see Fig. 6). With a maximum magnetic field of 14 gauss applied by the center coil (to simulate a uniform axial field), a field change of 0.45 gamma was observed at the Ames sensor. Using the upper coil to simulate a uniform transverse field, a field change of 27 gauss changed the field at the sensor by 31 gamma. Thus the field attenuation of the superconducting shield measured for the first case (center coil) was $3 \times 10^6$ and was $10^5$ for the second case. During the next attenuation test the Nb solenoid was left on while a 4.4-gauss field was applied with the 12-in. coil at the center of the 8-in. Linde dewar. The axial magnetic field was mapped before and during the field application. As shown in Fig. 14, field variations near the center of the superconducting shield were too small to be measured with the Ames sensor. Near the outer ends of the shield we could detect small field variations. The approximate logarithmic field attenuation for these points is also shown in Fig. 14 where we have plotted $\ell n$ (attenuation) versus Z, axial displacement from one end of the shield. The straight line plot suggests an attenuation relation of the form

$$A = \exp-(B+Z/r\ t)$$

where B = attenuation at Z = 0, i.e., one end of the shield; r = shield radius, and t = constant attenuation factor. From the data we find that B = 4.15 and t = 3.3. Thus the approximate attenuation per shield radius is $\exp(3.3) = 27/\text{radius}$. This agrees reasonably with our first measurements where the sensor was 6 radii in from the top of the shield and the measured attenuation was $3 \times 10^6$. Of course, for the present case, the Nb solenoid adds considerably to the shielding.

These attenuation measurements give a rough idea of the shielding to be expected from a superconducting cylinder but are not ideal. We do not have the facilities to apply uniform axial or perpendicular magnetic fields to the shield, and we were not able to lift the shield completely out of the cylindrical Mu-metal enclosure.

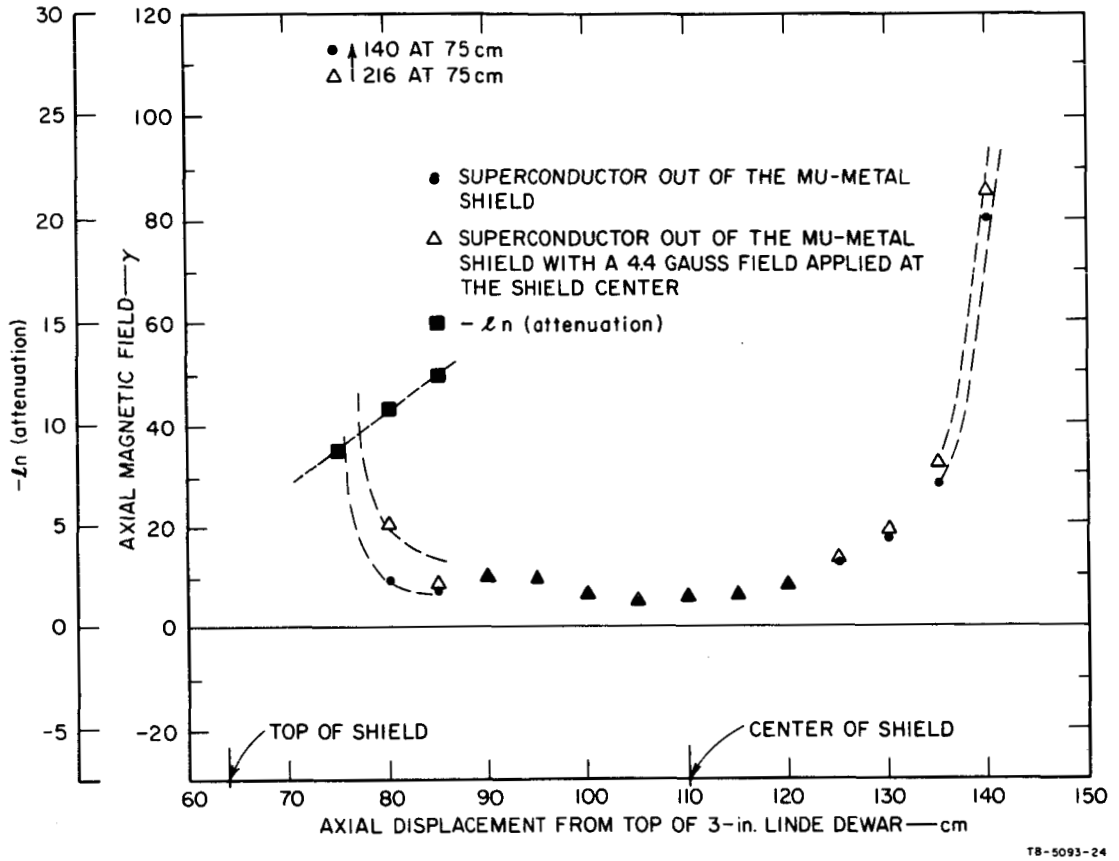


FIG. 14 ATTENUATION MEASUREMENTS OF THE SUPERCONDUCTING MAGNETIC SHIELD

## Long-Term Stability of the Ames Flux Gate Sensors

The magnetic shield facility has been used for four long-term stability tests of the Ames flux gate sensors. These tests lasted for 10, 5, 18, and 125 hours, respectively. The first three tests were made during a run when the Nb solenoid was inoperative and without making continuous records of external variables such as room temperature and external magnetic field. A single Ames sensor was used and it was mounted near the axial center of the superconducting shield. Figures 15 and 16 show the sensor reading versus time for these three tests, and Fig. 17 shows the axial magnetic field environment of each test. It is difficult to draw definite conclusions from these first three tests except that the sensor reading is not perfectly time-stable under the given test conditions.

The fourth stability test was instrumented to continuously record the sensor output from two Ames sensors mounted 30-cm apart as shown in Fig. 18. Also the following significant external variables were recorded:

1. Environmental air temperature of the sensors
2. Room temperature
3. Vertical component of the external magnetic field at the shield wall
4. Superconducting shield temperature
5. Output voltage from both sensor power supplies.

Due to the detail and complexity of this test it was described separately in an interim report submitted to Ames Research Center on August 23, 1965. A summary will be given here.

Each sensor reading was recorded on a strip recorder instrumented to automatically measure the recorder zero shift and gain every hour. The remaining variables were recorded on a multichannel Visicorder. Figure 19 is a greatly reduced plot of data taken from the continuous records. These plots were constructed by reading the original charts at intervals (1 to 5 min) required to accurately reproduce all variations, and plotting these points on a reduced time scale. Reading error for the sensors was $\pm\frac{1}{4}$ microgauss and this accounts for much of the breadth seen on the sensor plots. The air temperature shown in Fig. 19 is the air circulated by the sensors for temperature control and is directly proportional and approximately equal to the sensor temperature. The superconducting shield temperature did not vary more than $\pm 0.040^{\circ}C$ during the test; these data are not shown since intentional variations of as much as $0.5^{\circ}C$ had no measurable effect on the internal magnetic field. The two sensor supply voltage readings were plotted and showed a linear decrease in voltage with time which amounted to about 0.1 vdc over the full test. The initial voltage was 7.2 vdc. These data are not shown

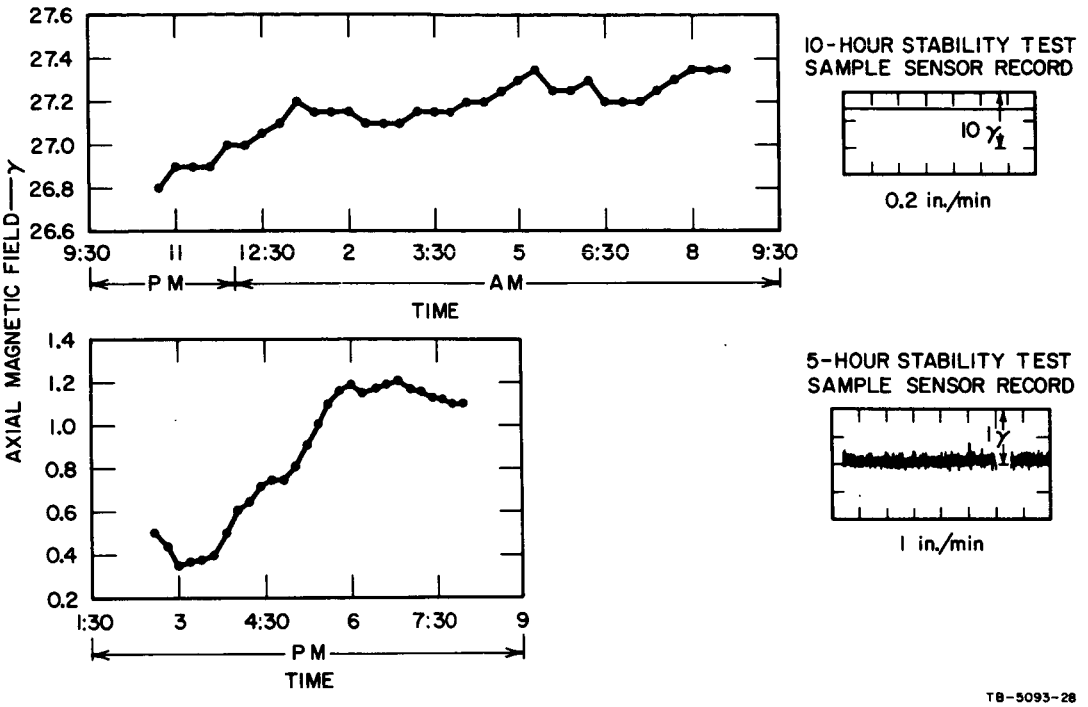


FIG. 15 PRELIMINARY LONG-TERM STABILITY TEST OF THE AMES SENSOR — 5 AND 10 Hr

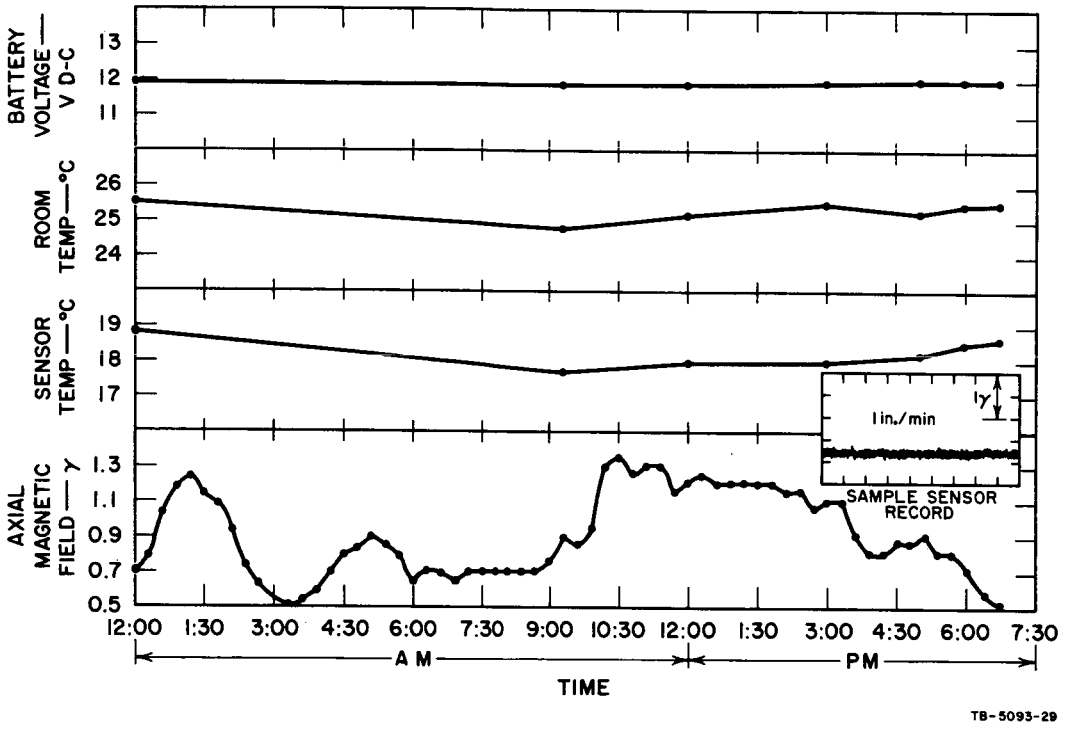


FIG. 16 PRELIMINARY LONG-TERM STABILITY TEST OF THE AMES SENSOR — 18 Hr

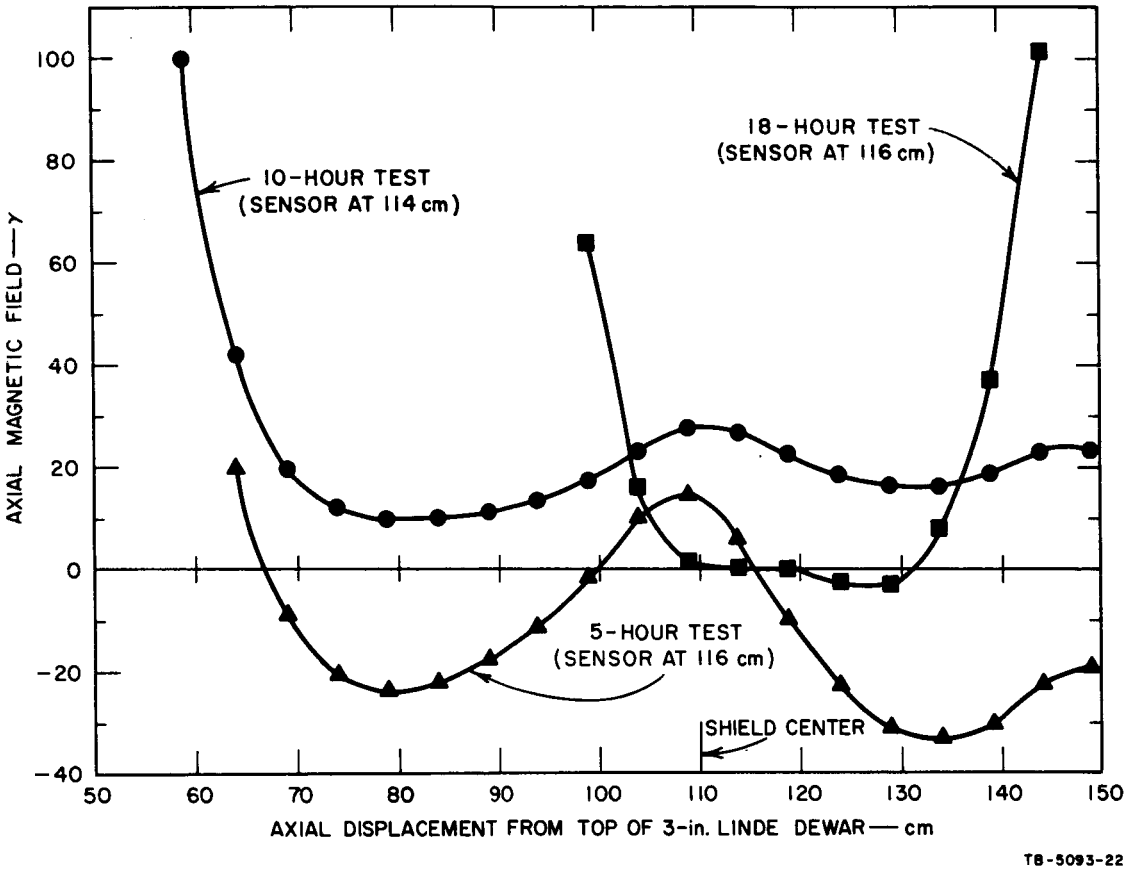


FIG. 17 AXIAL MAGNETIC FIELD MAPS PRIOR TO START OF PRELIMINARY STABILITY TESTS

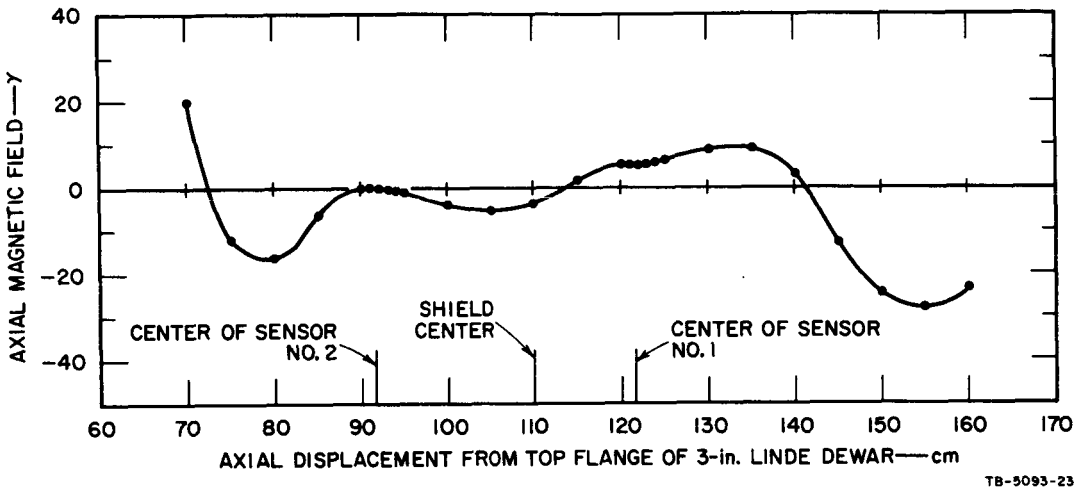


FIG. 18 AXIAL MAGNETIC FIELD MAP AND SENSOR LOCATIONS FOR LONG-TERM STABILITY TEST OF AMES SENSORS

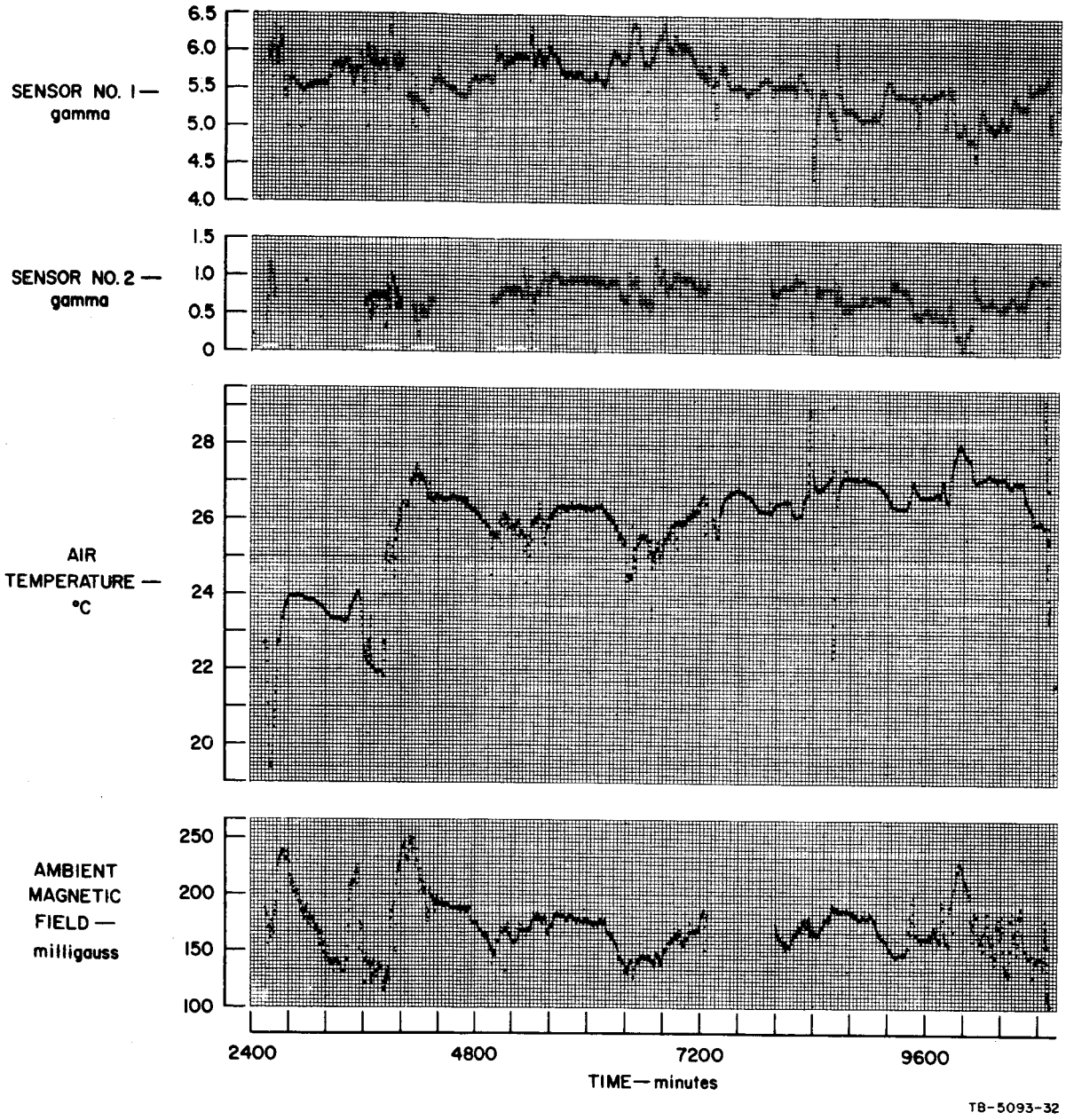


FIG. 19 LONG-TERM STABILITY TEST OF AMES SENSORS

due to the simple linear dependence. None of the recorded data have been omitted from the plots shown on Fig. 19. The regions where no points appear are regions where that particular channel was inoperative. The sensor air temperature was intentionally varied at the following times: 3665, 3690, 3830 to 3842, 4090, 7325, 7932, 8351, 8610, and 10890. At 3830 to 3842 the air control system was changed to cause a permanent shift in the average air temperature of about $2\frac{1}{2}^{o}$C. All of these temperature changes are reflected in the sensor readings. Also the ambient magnetic field readings are found to be closely correlated with the air temperature. Since the air temperature was equal to room temperature from time 3842 to the end of the test, except where the sensor temperature was intentionally varied, this suggests that the external magnetometer may be temperature sensitive. Measurements made after the stability test showed that the magnetometer, a Bell Model 240 differential gaussmeter, had a positive coefficient of 16.5 milligauss/$^{o}$C.

## Conclusions of the Long-Term Stability Test

The significant implications of this test are:

1. The superconducting magnetic shield and the Nb solenoid are extremely stable for long time periods, i.e., the magnetic field near the center of the shield is constant within the $\pm 1$ microgauss sensitivity of the Ames sensor for periods of at least one week and provide an excellent test environment for low field magnetometer studies.

2. The Ames flux gate sensors show very little long-term drift, and all measurable changes in the sensor readings are associated with a sensor temperature change.

These conclusions are based on a close examination of the data presented in Fig. 19, the sensor placement in the shield assembly, and the previously discussed superconducting shield attenuation measurements. The time interval from 2800 to 3250 shows large external magnetic field variations with constant sensor temperature and output. This indicates that the magnetic shield assembly is effective in shielding at least 100-milligauss external field variation, a result expected from the measured attenuation coefficients for the superconducting shield alone of at least $10^{5}$. Consideration of the placement of the sensors, given in Fig. 18, shows that the upper sensor was approximately $1\frac{1}{2}$ shield radii farther from the shield center than the lower sensor was. If the observed sensor variations were due to external field variations, then one would expect the variation in the lower sensor to be reduced by at least a factor of 30 over the upper sensor. This factor is derived from the attenuation measurements of the superconducting shield alone as previously discussed.

A region where all readings are constant is shown in Fig. 19 from time 5750 to 6150. It is clear from this interval that the sensor readings are constant within 0.1 gamma for almost 7 hours while the air temperature and ambient field were constant.

The intentional temperature variations, e.g., time 8400 in Fig. 19, indicate a negative sensor temperature coefficient. It was difficult to make meaningful estimates of the magnitude of the coefficient or the sensor equilibration time due to the method used in measuring and controlling the sensor temperature.

## Temperature Sensitivity of the Ames Sensors

Definite correlations between the temperature of the air used to regulate the sensor temperature and the sensor reading were observed during the long-term stability test. To investigate the nature of this temperature dependence and separate it from temperature variation of the Linde dewar wall, etc., we built the temperature control system shown in Fig. 20. In this apparatus the two sensors, each in a separate temperature controlled water bath, were placed 30-cm apart (as in the long-term stability test). The sensors were protected from direct water contact by thin rubber sleeves as shown in Fig. 20. The axial magnetic field of the superconducting shield immediately before the test is shown in Fig. 21.

During the test the lower sensor was kept at a constant temperature by circulating cold tap water ($22^{o}C$). The temperature of the upper sensor was varied from $21^{o}C$ to $55^{o}C$ by varying the amount of hot water that was mixed with cold water.

The actual sensor temperature was obtained from measurements of the resistance of the sensor feedback coil. To make this measurement the sensors were disconnected, one at a time, and the coil resistance was measured with an a-c bridge. Only a few microwatts of power are required for an accurate temperature measurement.

The temperature coefficient of the feedback coil of No. 1 sensor was measured by placing the sensor in thermal baths at known temperatures and measuring the coil resistance as above. The coefficient is constant at approximately $\frac{1}{2}$ ohm/$^{o}C$ over the range studied (from +20 to $55^{o}C$). Sensor No. 2 was not available at the time of these measurements but we assumed the two coefficients were approximately equal.

The sensor field sensitivity was measured frequently during the experiment by turning on a small field using the d-c transformer and the Nb solenoid of the superconducting magnetic shield assembly.

## Results

Figure 22 shows plots of the sensor reading, the sensor temperature, and the magnetic field sensitivity versus time. During the initial 40 to 50 minutes the water temperature and the sensor readings were not stable. The approximate temperature coefficients of Sensor No. 2 (the upper sensor) can be determined from Fig. 22. Figure 23 is the actual recorded trace of the No. 2 sensor for the time interval 95 to 124.

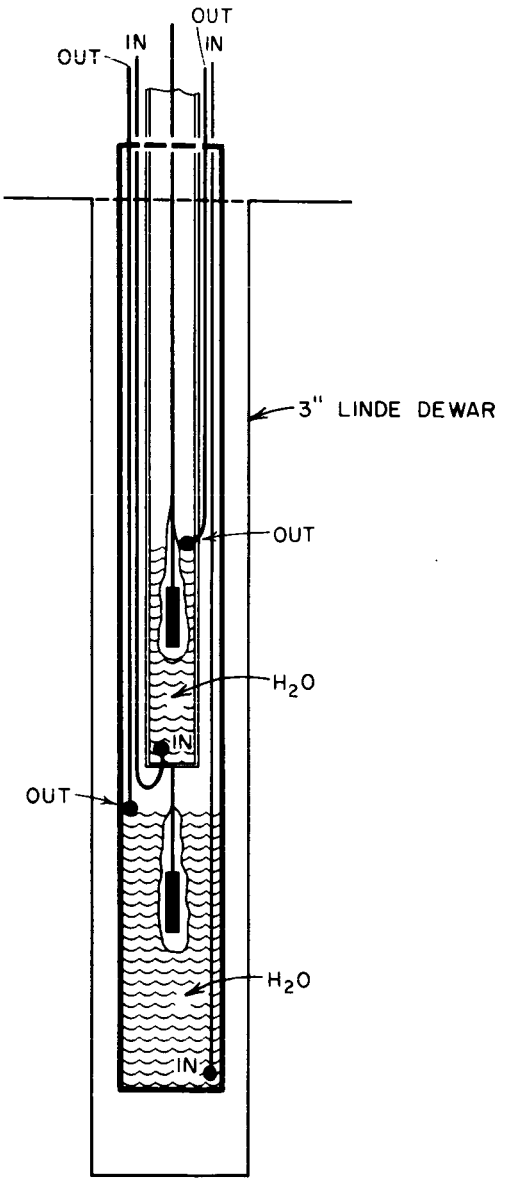


FIG. 20 SENSOR TEMPERATURE CONTROL SYSTEM

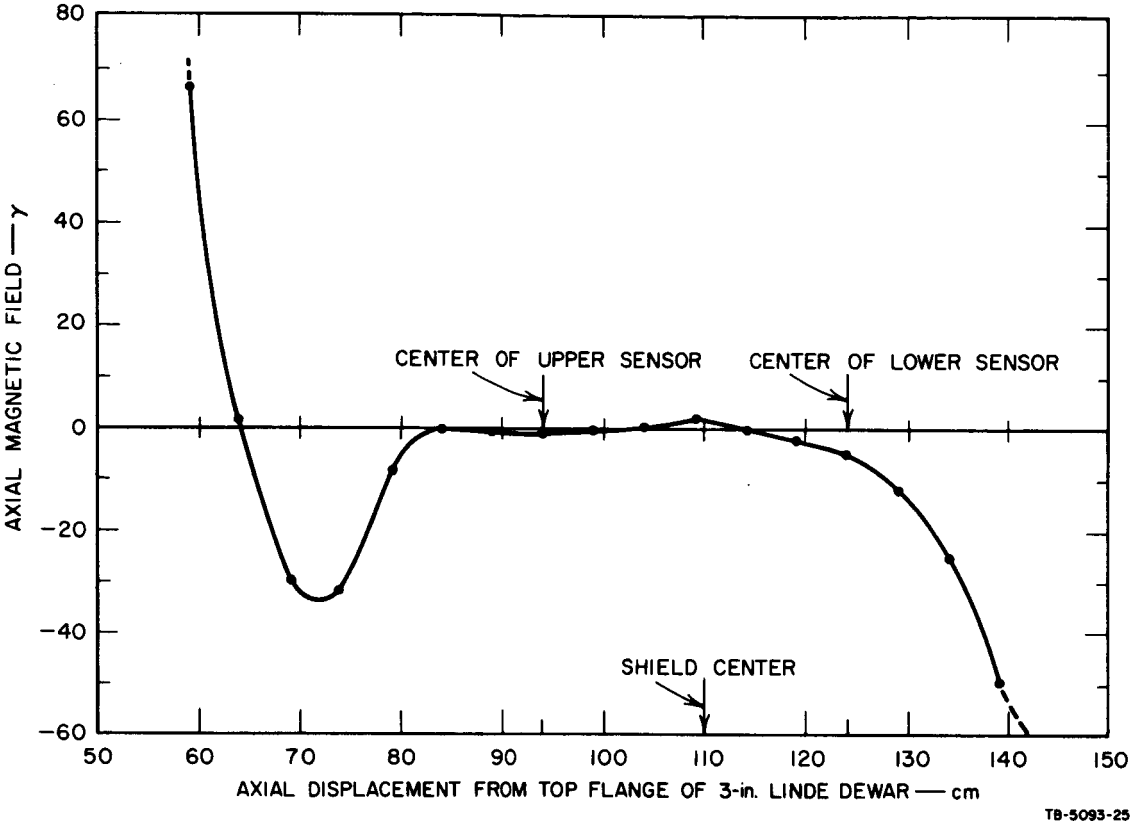


FIG. 21 AXIAL MAGNETIC FIELD AT THE BEGINNING OF THE TEMPERATURE SENSITIVITY TEST

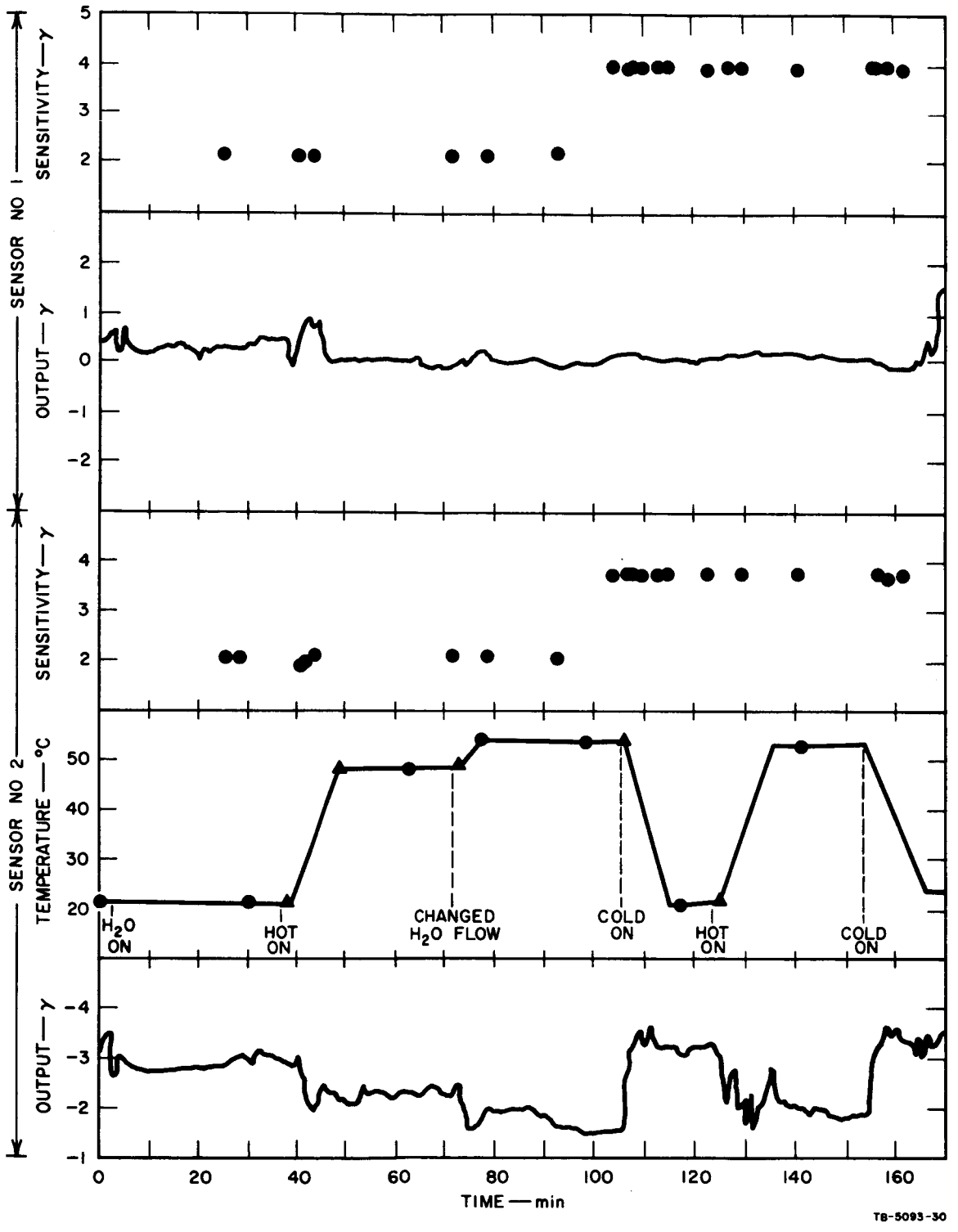


FIG. 22 DATA FROM THE TEMPERATURE SENSITIVITY TEST OF THE AMES SENSOR

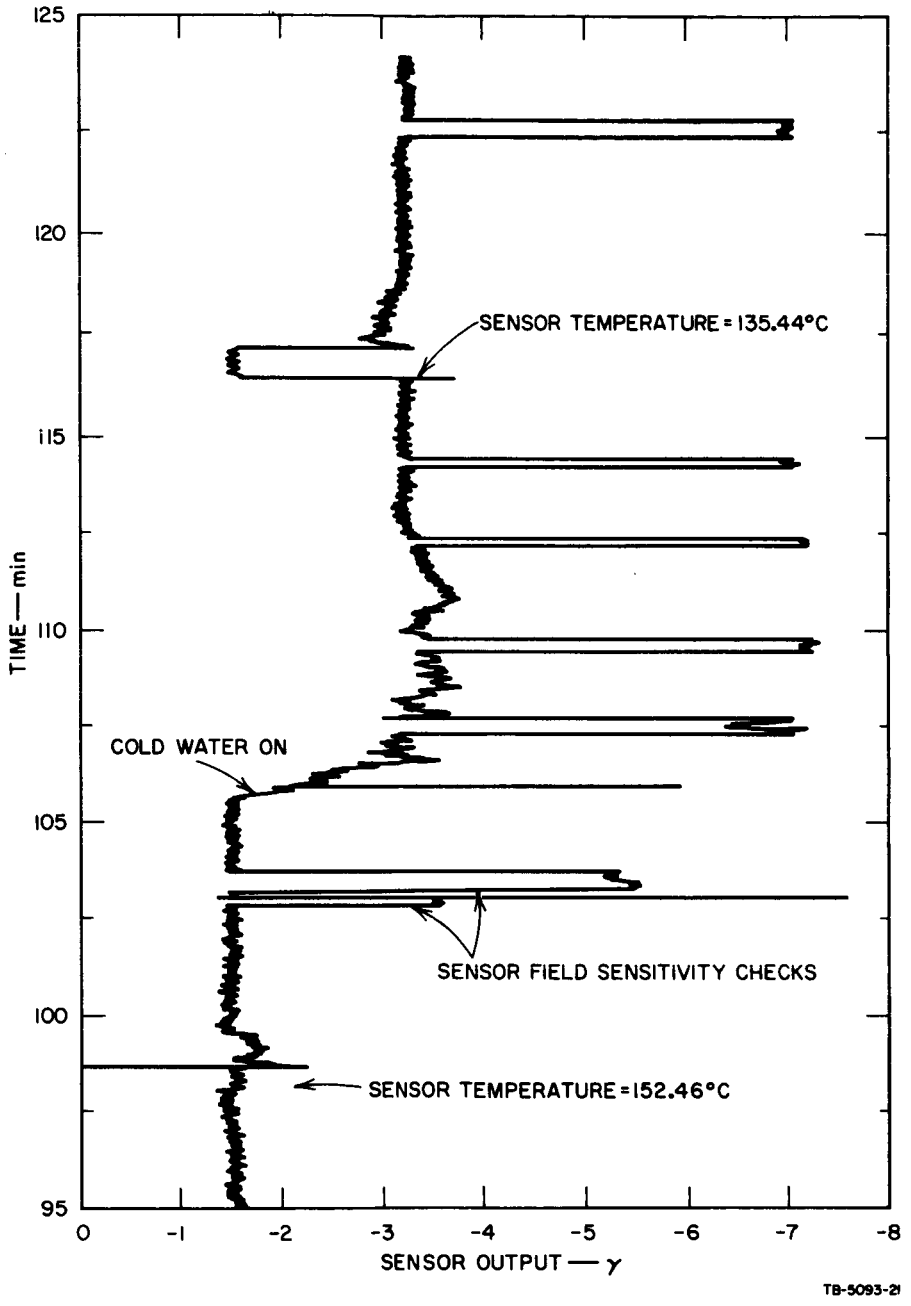


FIG. 23 RECORDER TRACE DURING TEMPERATURE SENSITIVITY MEASUREMENT OF AMES SENSOR NUMBER 2

This figure shows the equilibrium sensor record at two different temperatures, the region of temperature measurement, sensitivity measurements, and in particular, the increased noise during a temperature change.

The general conclusion reached from these data is that the Ames sensor output is sensitive to temperature. For large temperature changes ($\Delta T \simeq 30^{o}C$) the measured coefficient is approximately -0.4 $\mu$gauss/$^{o}$C.

## MEETING WITH HONEYWELL REPRESENTATIVES

On September 24, 1965, we had a discussion with Mr. Lutes and Mr. Jansson of Honeywell Company. The purpose of this discussion was to brief the Honeywell representatives on the design of our superconducting shield and suggest possible improvements which should be considered in future designs. This meeting was approved verbally by Dr. Debs and Mr. Munoz of Ames Research Center. A summary of our comments follows:

1. The magnetic field stability and attenuation of our shield is perfectly adequate to provide a suitable environment for testing flux gate sensors.

2. The rotation experiments performed with our shield have been inconclusive. We feel that a thicker lead coating and slower cooling rates through the superconducting transition temperature region would provide the expected eddy current cancellation of radial magnetic fields. Our existing shield assembly would be well suited for these studies.

3. Indium or tin would be superior to lead as a superconducting shield because they have much lower normal resistance immediately before the superconducting transition. The design of a long-term cryogenic environment for these lower temperature superconductors would be somewhat more involved but by no means impractical.

4. The cryostat designed for our shield assembly is satisfactory for most magnetometer and shielding experiments, and even for very long-term tests; but it has a rather large helium boil-off rate, about 0.5 liter/hr. We suggested an alternate design (Fig. 24) that should reduce the helium boil-off to about 1 liter/day. The significant features of this design are (a) all components are placed in the same vacuum space, so that thermal conduction heat leaks are minimized, and (b) all low temperature vacuum seals are eliminated. The detailed placement of components shown in Fig. 24 is for illustrative purposes only. Features such as efficient use of the cold helium boil-off vapor, radiation shielding, transfer lines, possible omission of the nitrogen shield etc. were not considered in this preliminary suggestion.

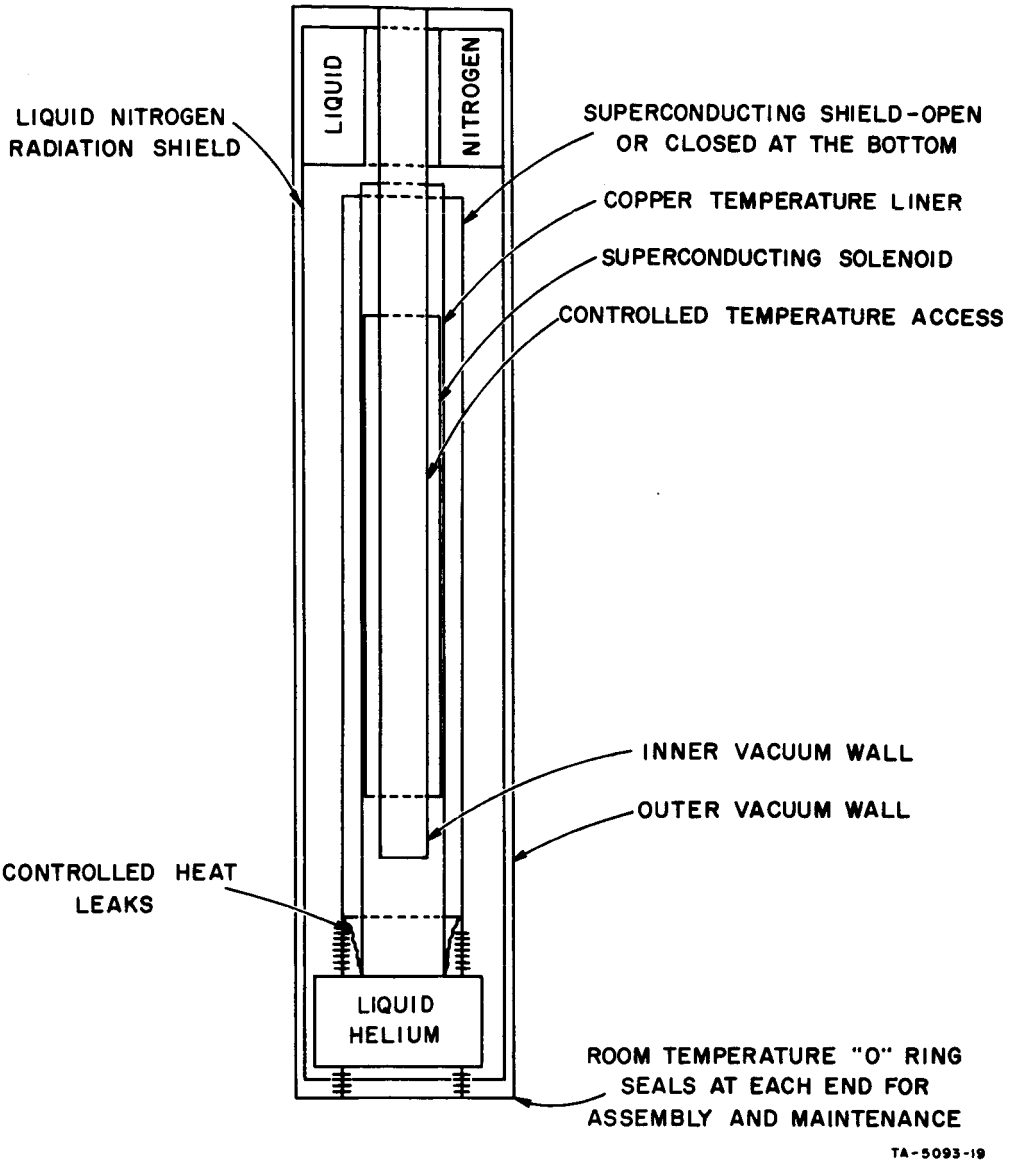


FIG. 24 SUGGESTED SUPERCONDUCTING MAGNETIC SHIELD DESIGN

## FUTURE WORK

Our immediate efforts are devoted to the development of the quantized flux magnetometer. In the next magnetometer experiment we will attempt to optically heat the superconducting modulator with a chopped light beam. (This approach was selected, upon our recommendation, in a meeting with Dimeff, Debs, Gardner, and Murphy of Ames Research Center on July 20, 1965.) Figure 25 shows a sketch of the experimental set up. Assembly of this apparatus has been delayed due to difficulty in having the optical surfaces of the $\frac{1}{8}$-in. quartz light pipe properly machined and polished. The indium modulator has been vapor deposited and is ready to mount. We expect that assembly will be complete and the first run will be conducted during the month of October.

Future tasks are to (1) measure the appropriate circuit parameters necessary to optimize the superconducting magnetometer circuit design, (2) investigate the absolute field measuring characteristics of the superconducting circuits, and (3) consider other instrumental applications. These applications will utilize the Josephson effect; the London moment; and the three effects exploited in this magnetometer development, namely, quantized flux, zero resistance, and the Meissner effect.

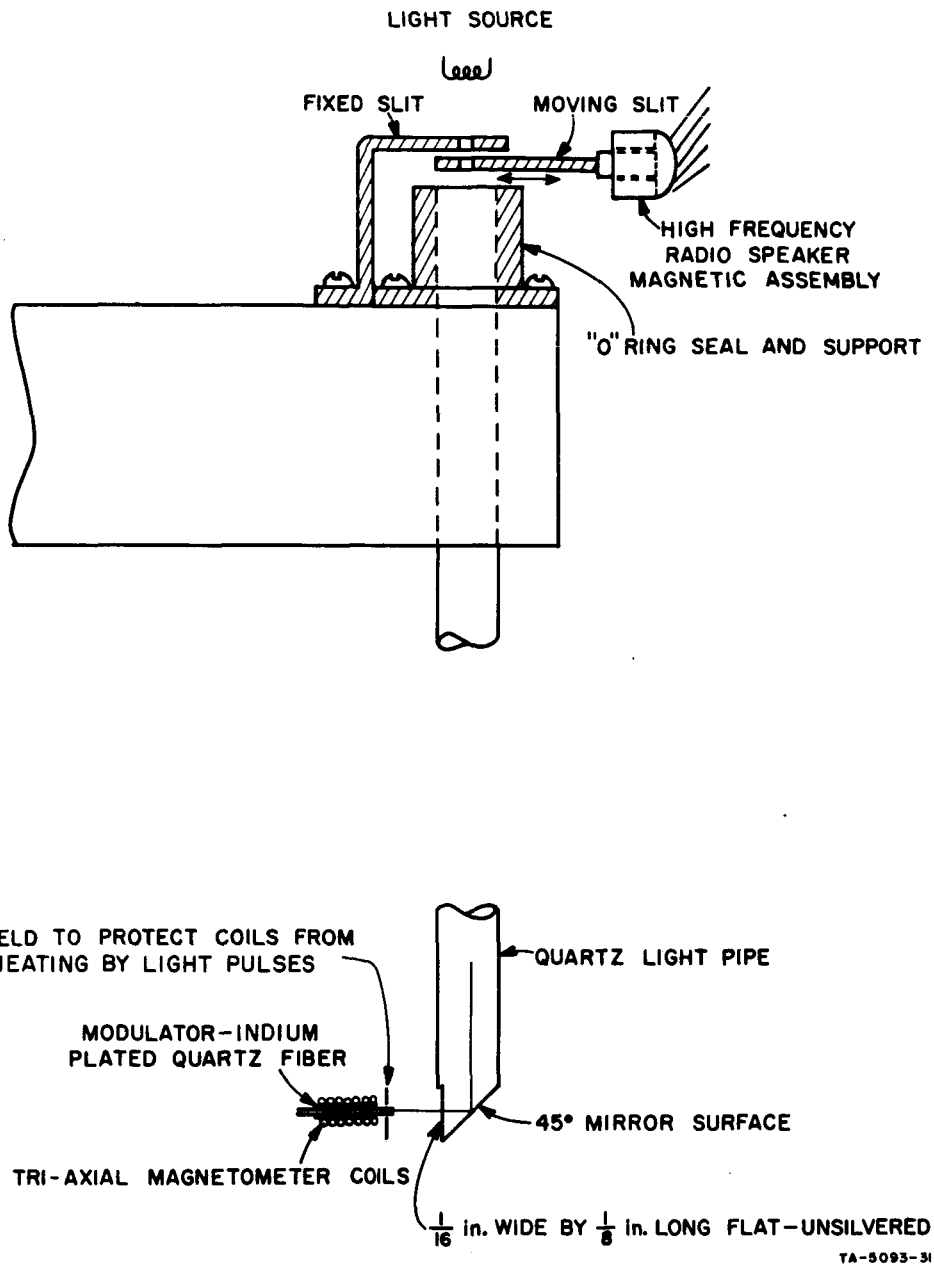


FIG. 25 LIGHT PIPE FOR OPTICAL MODULATION EXPERIMENT

(a) Upper end of magnetometer assembly as modified for the quartz light pipe. Refer to Fig. 5 for complete magnetometer assembly.
(b) Lower end of magnetometer assembly showing enlarged view of modulator and quartz light pipe.